REMOTE SENSING AND SIMULATION TO ESTIMATE FOREST PRODUCTIVITY IN SOUTHERN PINE PLANTATIONS

By

DOUGLAS A. SHOEMAKER

A THESIS PRESENTED TO THE GRADUATE SCHOOL
OF THE UNIVERSITY OF FLORIDA IN PARTIAL FULFILLMENT
OF THE REQUIREMENTS FOR THE DEGREE OF
MASTER OF SCIENCE

UNIVERSITY OF FLORIDA

2005

This research is dedicated to my mother and father.

ACKNOWLEDGMENTS

I am grateful for the opportunity to work with Dr. Wendell Cropper who was generous with his knowledge, which is substantial, and patience. I also thank committee members Tim Martin and Michael Binford for access to valuable data.

I am obliged to Dr. Jane Southworth whose unbiased eye and fearless commentary kept me honest.

I want to acknowledge individuals who contributed in large and small ways to this work including Dr. Timothy Fik for inspiration in statistics; Alan Wilson and Brad Greenlee of Rayonier Inc., landholder of the study site and member of the FBRC; Greg Starr for helping review this manuscript; and Dr. Loukas G. Arvanitis who kept me on task.

Special thanks go to fellow students Louise Loudermilk and Brian Roth who remain steadfast allies.

TABLE OF CONTENTS

LIST OF TABLES

Table page

LIST OF FIGURES

Abstract of Thesis Presented to the Graduate School
of the University of Florida in Partial Fulfillment of the
Requirements for the Degree of Master of Science

REMOTE SENSING AND SIMULATION TO ESTIMATE FOREST PRODUCTIVITY IN SOUTHERN PINE PLANTATIONS

By

Douglas A. Shoemaker

August, 2005

Chair: Wendell P. Cropper, Jr.
Major Department: Forest Resources and Conservation

Pine plantations of the Southeastern United States constitute one-half of the world's industrial forests. Managing these forests for maximum yield is a primary economic goal of timber interests; the rate at which these forests remove and sequester atmospheric carbon as woody biomass is of interest to climate change researchers who recognize forests as the only significant human-managed sink of greenhouse gases.

To investigate a given pine plantation's productivity and corresponding ability to store carbon two significant parameters were predicted: net ecosystem exchange (NEE) and leaf area index (LAI). Measurement of LAI *in situ* is laborious and expensive; extraction of LAI from satellite imagery would have the advantages of making predictions spatially explicit, scalable, and would allow for sampling of inaccessible areas. Consequently the study was conducted in three steps: 1) the development of an LAI extraction model using satellite imagery as a primary data source, 2) application of the model to a study extent, and 3) determination of NEE using derived LAI values and Cropper's SPM-2 forest simulation model.

We derived several models for extracting LAI values using various prediction techniques. Of these a best model was selected based on performance and potential for operational application. The generalized southern pine LAI predictive model (GSP-LAI) was developed using artificial neural network (ANN) multivariate regression and incorporating important local information including phenological and climatic data. In validation tests the model explained > 75% of variance ($r^2 = 0.77$) with an RMSE < 0.50.

The GSP-LAI model was applied to Landsat ETM+ image recorded September 17, 2001, of the Bradford forest, north of Waldo, FL. Within the extent are substantial slash (*Pinus elliottii*) and loblolly (*P. taeda*) pine plantations. Based on image and stand data projected LAI values for 10,797 ha (26,669 acres) were estimated to range between 0 and 3.93 $m^2\ m^{-2}$ with a mean of 1.53 $m^2\ m^{-2}$. Input of slash pine LAI values into SPM-2 yielded estimates of NEE for the area ranging from -5.52 to 11.06 Mg $ha^{-1}\ yr^{-1}$ with a mean of 3.47 Mg $ha^{-1}\ yr^{-1}$. Total carbon sequestered for the area analyzed is 33,920 metric tons, or approximately 1.4 tons per acre.

Based on these results a map of the Bradford forest was drawn locating areas of carbon loss and gain and LAI values for individual stands. Ownership and accounting of carbon stores are prerequisites to anticipated carbon trading schemes. The availability of stand-level LAI values has significance for forest managers seeking to quantify canopy response to silvicultural treatments. Efficiencies may be realized in management practices which optimize leaf growth based on site potential rather than focusing on resource availability.

CHAPTER 1
BACKGROUND

The monitoring of forest biological processes has become increasingly important as nations seek to control their outputs of carbon dioxide (CO_2), the primary component of climate-changing greenhouse gasses, in the face of global climate change. Forests in general and trees specifically provide the essential service of removing CO_2 from the atmospheric reservoir of carbon through photosynthesis, where carbon is fixed as energy-storing sugars. The metabolic processes of the tree respire carbon back to the atmosphere but a portion is isolated from environment in the durable biomass of the plant, namely wood. Carbon will re-enter the atmosphere when wood decomposes or burns, however the period of carbon sequestration is on the terms of decades, perhaps longer if that wood is built into a structure or buried as waste in a landfill.

Carbon sequestration via forestry is currently the only means by which mankind can significantly remove carbon from the atmosphere; agricultural plantings are not counted as the carbon returns to the environment too quickly to have an appreciable effect (Tans & White 1998). The Kyoto Protocol of 1997, an international accord which seeks to reduce the emissions of greenhouse gasses, calls for the cooperation of nations in finding and maintaining sinks, or reservoirs, of greenhouse gases. This language lays the foundation for the trade in carbon credits, whereby a nation exceeding its emissions of CO_2 could pay another nation to sequester carbon, *e.g.*, let stand a forest scheduled for harvest. The emissions trading scheme (ETS) identifies value (and a potential new revenue source) from what was previously an un-valued, non-market services provided

by the forest. Carbon credits are not simply economic talk—on October 1, 2003, carbon credits traded for the first time in an international market, the Chicago Climate Exchange, for $.98 per metric ton (Doran, 2003).

Modeling and Leaf Area Index

Economists and ecologist want to better understand the flow of carbon in and out of forests on a regional and global scale. Forest ecosystems are complex, and systems ecologists use models to analyze the responses and productivity of forests, especially the movements of carbon (Waring & Running 1998). Models such as SPM-2 aim to characterize the flows of carbon between the atmosphere, the trees and the soil (Cropper 2000). This model, specific to coastal plain slash pine (*Pinus elliottii*) forests, uses dozens of input parameters ranging from rainfall and humidity to wind speed; outputs include carbon assimilation (g CO_2 m^{-2} d^{-1} and Mg C ha^{-1} yr^{-1}) and annual stem growth (g m^{-2}).

In forest system models the complexities of leaf area, including canopy structures and geometry, may be simplified into a ratio of total leaf area to unit ground area known as the leaf area index (Waring & Running 1998). This leaf area index (LAI) composes the most basic input into current forest system models (Stenberg *et al*. 2003).

Unfortunately LAI is notoriously difficult to determine for a number of logistical reasons to be illustrated and for many species it changes within the growing season. In the subject species *P. elliottii*, LAI varies seasonally because trees bear two age classes of leaves through most of the year. A maximum LAI occurs around mid-September when last year's leaf class has not yet senesced and the new leaves have reached their maximum elongation. Workers thus need to be aware of the time-of-year when the sample is taken and account for this seasonal variation (Gholz *et al*. 1991). The climatic

conditions at time of sampling are also important, as drought or leaf loss due to storms can depress the index.

LAI is measured *in situ* three distinct ways: the area-harvest method, the leaf litter collection method, and the canopy transmittance method. A fourth indirect method involves the use of satellite imagery to measure electromagnetic energy reflected from the forest canopy at specific indicative wavelengths. Though laborious and limited in spatial extent, *in situ* methods provide important ground truth estimates for validating and training remote sensing techniques (Stenberg *et al*. 2003).

The area-harvest method involves randomly choosing a tree in a forest community similar to that of the study, measuring the footprint of the tree, harvesting it, and giving each leaf collected a specific leaf area (SLA), which is the ratio of fresh leaf area to dry leaf mass. Age class of leaves should be accounted for as SLA can differ by a factor of two between old and new foliage. The number of trees measured in this fashion should reflect a sample size sufficient to represent the spatial heterogeneity of community studied (Stenberg *et al*. 2003).

The leaf litter collection method involves a sample selection process similar to the area-harvest method, however leaves are continuously collected in leaf traps and each assessed as to area and age class. Extrapolation techniques then extend the information along a timeline to determine LAI at a given time (Stenberg *et al*. 2003).

Field determinations of LAI may also be made without laborious collection using the canopy transmittance method. Optical sensors that measure light not intercepted by leaves, or canopy gap, are placed beneath the canopy. The amount of light recorded is then compared with a model of canopy architecture, and from there an LAI is derived (Stenberg *et al*. 2003). This method assumes the distribution of leaves in the canopy to be

random; thus it is invalid for open-canopy forests, such as coniferous forests (Gholz *et al*. 1991).

In situ LAI determinations are the standard of comparison for all new techniques, and are currently the most reliable data available. Area-harvest methods and leaf litter collection are assumed to be more accurate than canopy transmittance methods, however Gower reports that all *in situ* methods are within 70% to 75% accurate for most canopies, exceptions being non-random leaf distributions and LAI > 6 (Stenberg *et al*. 2003).

Use of Remote Sensing Data

Because of the arduous nature of determining LAI *in situ* there has been emphasis on developing new methods which use remotely sensed data captured by sensors on airborne or satellite platforms (Gholz *et al.* 1991; Sader *et al.* 2003). These methods take advantage of the fact that photosynthetically active vegetation absorb specific wavelengths of the incident electromagnetic (EM) spectrum and reflect others. Specifically, blue (0.45-0.52 μm) and red (0.63-0.69μm) are absorbed, green (0.53-0.62μm) and near infrared (0.7-1.2 μm) are reflected (Jensen 2000). Reflectance of green wavelengths creates the green appearance of foliage, while reflected NIR is invisible to the human eye. Measurements of absorbance and reflectance comprise unique spectral signatures that distinguish between vegetation and other ground features, or between different genera of plants.

The reflectance of NIR bandwidths are of particular interest as they are indicative of the amount of leaves within the canopy at the time of imaging. Reflected wavelengths consist of EM energy the plant cannot use which leaves reflect or allow to pass through (transmit). Transmitted radiation falls incident on a leaf below, which in turn reflects

50% and transmits 50%. This characteristic is called the leaf additive reflectance, and it is indicative of amount of leaves within a canopy.

Several remote sensing indices have been created to classify and measure foliage from space using the differential reflectance and absorption characteristics of red and near infrared bandwidths. The most widely used algorithms (Trishchenko *et al*. 2002) include Simple Ratio (Birth & Mcvey 1968) and Normalized Difference Vegetative Index (Eklundh *et al*. 2003). The formula for Simple ratio (SR) is described as:

$$SR = NIR/red$$

Normalized Difference Vegetative Index (NDVI) is described as:

$$NDVI = (NIR - red) / (NIR + red)$$

The ratios have the advantage of using two of the seven or more bands typically collected, and requiring no other auxiliary data for calculation. However, they require calibration from *in situ* reference locations in order to produce secondary data, such as physical measurements of biomass (Wood *et al*. 2003). Additionally, variability is introduced to the index by soil reflectance, atmospheric effects, and instrument calibration (Holben *et al.* 1986; Huete 1988). Of these three soil reflectance is pervasive and its contribution to vegetation indices is ideally subtracted using a two-stream solution developed by Price (Soudani *et al*. 2002).

A Leaf area index is a secondary datum produced by linking *in situ* reference data with a vegetation index, typically NDVI (Sader *et al*. 2003). The data are connected through regression analysis resulting in a linear relationship (Ramsey & Jensen 1996).

Scale and Resolution

The use of satellite imagery has also brought the issue of scale to the forefront. The spatial extent of forest systems modeled has typically been limited to a stand or woodlot

scale due to the restrictive nature of *in situ* LAI sampling. Estimates of LAI from satellite imagery may be the only way to measure vegetative processes of forest at a regional or larger scale (Sader *et al*. 2003). A fundamental question in choosing a data source is one of resolution. In remotely sensed data, a pixel, or picture element, represents a spatial extent on the ground that is the minimum area capable of resolution by a particular sensor. For the Thematic Mapper (TM) carried by the satellite platform Landsat the pixel size is a 30 meter by 30 meter square. Thus the resolution of Landsat TM is said to be 30 meters. Different sensors have different resolutions. The French SPOT satellite carrying the High Resolution Radiometer (HRR) has a 10 meter resolution (Jensen 2000). In working with vegetation, resolution should match the size of the feature-of-interest as closely as possible.

CHAPTER 2
PREDICTION OF LEAF AREA INDEX FOR SOUTHERN PINE PLANTATIONS FROM SATELLITE IMAGERY

Introduction

Pine plantations of the Southeastern United States constitute one-half of the world's industrial forests. In Florida alone annual timber revenue exceeds $16 billion and is the dominant agricultural sector (Hodges *et al*. 2005). Managing these forests for maximum yield is a primary economic goal of timber interests; the rate at which these forests remove and sequester atmospheric carbon as woody biomass is of interest to climate change researchers who recognize forests as the only significant human-managed sink of greenhouse gases.

Leaf area index (LAI) is a key parameter for estimation of a given pine plantation's productivity or net ecosystem exchange of carbon (NEE). In this study we focus on the estimation of LAI, a primary biophysical parameter used in forest productivity modeling, carbon sequestration studies, and by forest managers seeking to quantify canopy responses to silvicultural treatments (Cropper & Gholz 1993; Sampson *et al.* 1998; Gower *et al.* 1999; Reich *et al.* 1999). LAI is the ratio of leaf surface area supported by a plant to its corresponding horizontal projection on the ground, and it is difficult and expensive to assess *in situ* resulting in sparse sample sets that are necessarily localized at a stand scale and thus difficult to extrapolate to larger extents (Fassnacht *et al*. 1997).

Determination of LAI from remotely sensed data would have the advantage of being spatially explicit, scaleable from stand to regional or larger extents, and could

sample remote or inaccessible areas (Running *et al*. 1986). An ideal empirical model linking ground-referenced LAI to remote sensing data would make reliable predictions at various extents and image dates and be general enough to incorporate important local information such as climatological and phenological data.

As Gobron *et al*. (1997) point out the range of variation that exists in vegetative biomes of interest worldwide preclude the likelihood of a single universal relationship between LAI and remote sensing products; but regional prediction of LAI in important subject systems such as the extensive and economically important holdings of industrial pine plantations across the southeastern U. S. should have important applications.

There have been previous attempts to remotely estimate LAI for this specific forest system. Industrial plantations in the south typically consist of dense plantings of loblolly (*Pinus taeda*) and slash (*Pinus elliottii*) pine (Prestemon & Abt 2002). Gholz, Curran *et al* (1991) studied a north-central Florida mature slash pine plantation where they evaluated LAI determination techniques and related those to remote sensing data collected by Landsat TM. Flores (2003) looked at loblolly pine in North Carolina and related ground-based indirect LAI values to hyperspectral remote sensing data.

These studies used ordinary least squares (OLS) regression analysis to establish an empirical relationship between vegetative indices (VI) and ground-referenced LAI. The best understood VIs are the normalized difference vegetative index (NDVI) (Rouse *et al*. 1973) and the simple ratio (SR) (Birth & Mcvey 1968) both of which make use of recorded values for red and near infrared wavelengths. In the case of Gholz *et al* (1991) three predictive equations were produced using NDVI. Flores used SR in his predictor. We evaluated these models using a new dataset assembled for this study and found none

exhibited significant predictive ability (see Table 2-2 in results). While linear regression remains a popular approach, variations in surface and atmospheric conditions as well as the structural considerations of satellite remote sensing have foiled attempts to establish a universal relationship between LAI and VIs (Gobron *et al.* 1997; Fang & Liang 2003).

Perhaps this failure is due to under- or misspecification of the models. The biochemical and structural component of the forest canopy is complex, varying in both time and locale (Raffy *et al*. 2003). Cohen *et al* (2003) suggest that the incorporation of other recorded spectra and the use of data from multiple dates as predictive variables as a way to improve regression analysis in remote sensing. Multivariate regression techniques allow for the incorporation of more types of data, including important locational information such as climate or categorical stand data. When OLS regression is used variable selection techniques permit the exploration of a wide range of data for significance.

Despite these advantages many of the assumptions necessary for OLS regression are violated by remote sensing data which characteristically exhibits non-normality and tends to suffer multicollinearity and autocorrelation. For these reasons a nonparametric technique, regression with artificial neural networks, was investigated as an alternative to OLS regression.

Artificial neural networks (ANN) are loosely modeled on brain function: a series of nodes representing inputs, outputs and internal variables are connected by synapses of varying strength and connectivity (Jensen *et al*. 1999). The network architecture is typically oriented as a perceptron which ‘learns’ by passing information from inputs to outputs (forward propagation) and from output to inputs (back propagation) to optimize

the accuracy of prediction by adjusting weights. The ability to accommodate complexity can be made by altering the construction of the network to include multiple layers of internal nodes. These networks are attractively robust in that many of the assumptions needed for OLS regression are relaxed, including requirements of normality and independence.

In this study our objective was to develop a single 'general' empirical model capable of producing reliable LAI predictions at various extents and image dates. We hypothesized that such a solution would require multivariate statistics to incorporate important local information such as climatological and phenological data. Three regression techniques, linear OLS, multiple OLS and ANN, were applied to a large dataset constructed from data acquired by Landsat sensors over a 10 year period , and the resultant models evaluated for performance using a validation process. Models were developed in strata of increasing complexity to identify high performing yet simple solutions.

Methods

Study Sites

Two plantations of southern pine were used in this study: the Intensive Management Practices Assessment Center (IMPAC) operated by the Forest Biology Research Cooperative (FBRC) and the Donaldson tract, part of the Bradford forest owned by Rayonier, Inc. and site of a Florida Ameriflux eddy covariance monitoring station. Both sites are planted with southern pine species loblolly (*Pinus taeda* L.) and slash (*Pinus elliottii* var. *elliottii*) which have similar physiology and seasonal foliage dynamics (Gholz *et al*. 1991).

The IMPAC site is located 10 km north of Gainesville, Florida USA (29° 30′ N, 82° 20′ W, Figure 2-1.) The site is flat with elevation varying < 2 m and experiences a mean annual temperature of 21.7°C and 1320 mm annual rainfall. Soils are characterized as sandy, siliceous hyperthermic Ultic Alaquods (Swindle *et al*. 1988). The stand was established in 1983 at a stocking rate of 1495 seedlings per hectare, a dense planting typical of industrial pine plantations. The site was surveyed using a differentially corrected global positioning system (DGPS) in February, 2004.

The site consists of 24 study plots, each 850 m², exhibiting factorial combinations of species (loblolly and slash pine), fertilization (annual or none) and control of understory vegetation (sustained or none) in three replicates. Fertilization of respective plots occurred annually for ages 1-11, was ceased for ages 12-15, and resumed at age 16.

The Donaldson tract is located 12 km east of the IMPAC site (29° 48′ N, 82° 12′ W) the stand was established in 1989 and stocked at a rate of 1789 slash pine seedlings per hectare. The site is flat and well drained. Within the stand are four 2,500 m² plots from which leaf litterfall was collected starting at age 10 (1999). Plots were surveyed with GPS May, 2002. Estimates of LAI based on needlefall from 10 randomly located traps were collected by Florida Ameriflux averaged into a single value for all four plots beginning April, 1999.

Remote Sensing Data

The study acquired 18 cloudless images recorded of the study area between 1991 and 2001 by the Landsat 5 and 7 satellite platforms (Table 2-1.). This series of images contain examples of each of the four phenological categories and is concurrent with cycles of dry and wet periods for the region (Figure 2-2).

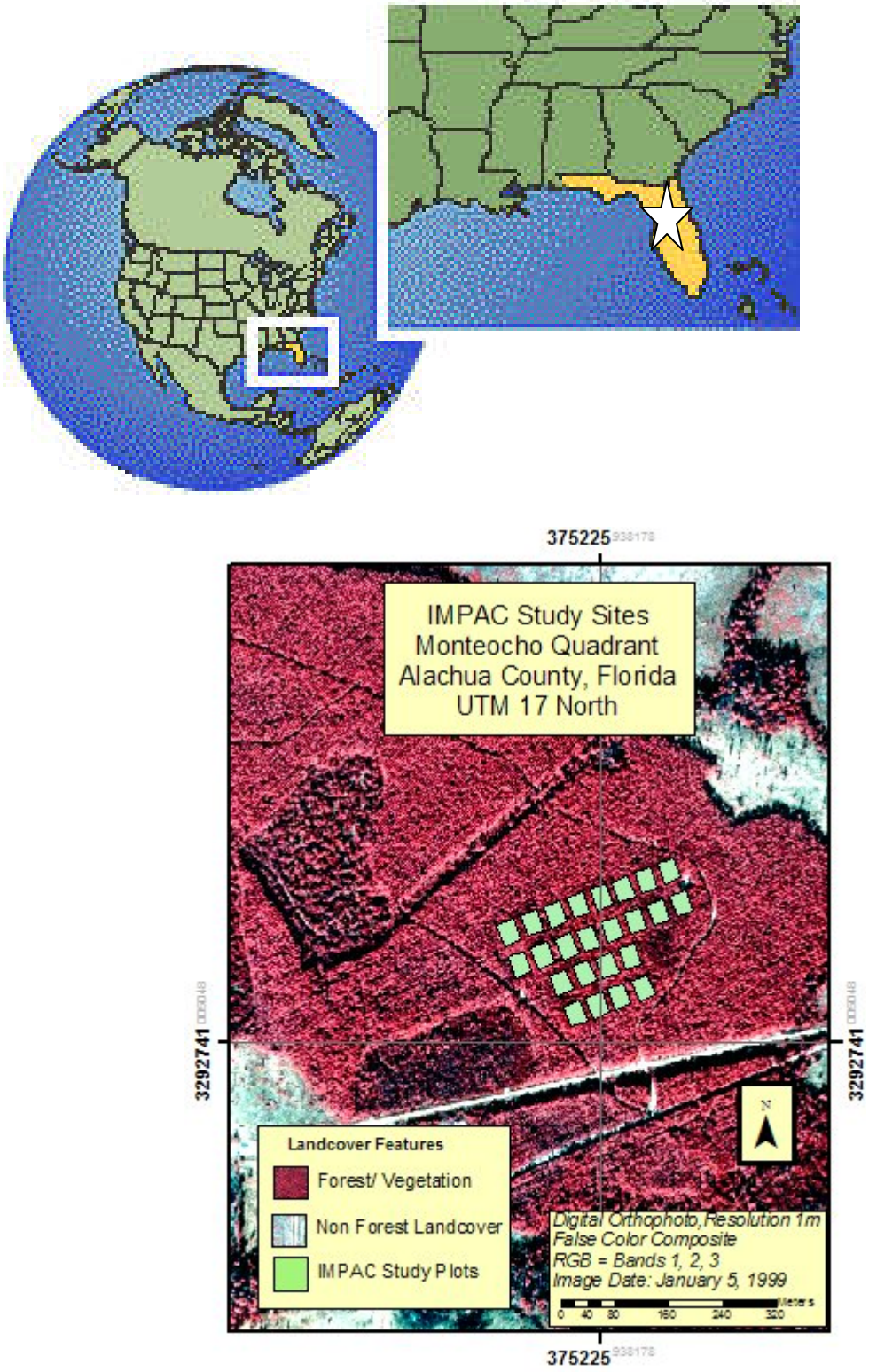

Figure 2-1. Map of the Intensive Management Practices Assessment Center, Alachua County, Florida, USA.

Table 2-1. Catalog of images used in study.

Number	Image Date†	Sensor	Phenological period	PHDI‡
1	1/17/91	TM	Declining LAI	-1.75
2	3/22/91	TM	Minimum LAI	-0.63
3	10/16/91	TM	Declining LAI	2.63
4	1/20/92	TM	Declining LAI	1.59
5	8/31/92	TM	Maximum LAI	1.22
6	3/27/93	TM	Minimum LAI	1.85
7	8/18/93	TM	Maximum LAI	-2.76
8	1/25/94	TM	Minimum LAI	2.78
9	9/6/94	TM	Maximum LAI	1.3
10	6/7/96	TM	Expanding LAI	0.83
11	9/30/97	TM	Maximum LAI	-0.86
12	6/29/98	TM	Expanding LAI	0.59
13	1/7/99	TM	Minimum LAI	-1.9
14	9/4/99	TM	Maximum LAI	-2.38
15	1/2/00	ETM+	Declining LAI	-2.29
16	4/7/00	ETM+	Minimum LAI	-2.71
17	8/13/00	ETM+	Maximum LAI	-4.02
18	1/4/01	ETM+	Declining LAI	-3.05

† All images are Path 17N, row 39. Datum NAD83/GRS 80. Georectification error ±0.5 pixels
‡ Palmer hydrological drought index: negative values indicate dry conditions, positives wet, normal ≈ 0. National Climatic Data Center.

Images were captured with the both the Thematic Mapper (TM) sensor aboard Landsat 5 and the Enhanced Thematic Mapper Plus (ETM+) aboard Landsat 7. These sensors are functionally identical for the bandwidths used in the study: visible spectra blue (0.45 – 0.52 μm, band 1), green (0.52 – 0.60 μm, band 2) red (0.60 – 0.63 μm, band 3) and infrared spectra: near (0.69 – 0.76 μm, band 4) mid (1.55 – 1.75 μm, band 5) and reflected thermal (2.08 – 2.35 μm, band 7). Spatial resolution for these bands is 30m. Band 6, which detects emitted thermal radiance between 10.5 – 12.5μm, has a resolution of 120 m for TM and 60m for ETM+.

Brightness values (BV) were recovered from the data based on the center point of each study plot. All images were individually rectified using a second order polynomial equation with between 30 and 40 ground control points; while the images maintained the

accepted rectification accuracy of ±0.5 pixels the overlay with study plots varied from image to image.

Seasonal LAI Dynamics and Leaf Litterfall Data

P. taeda and *elliottii* are evergreen trees that maintain two age classes of leaves throughout much of the year, needles from both the previous and current growing seasons (Gholz *et al.* 1991; Curran *et al.* 1992; Teskey *et al.* 1994). In north Florida these classes overlap between July and September, establishing a period of peak leaf area categorized as maximum LAI. As such the phenological year is typically categorized into four periods: minimum LAI, leaf expansion, maximum LAI and declining LAI (Figure 2-3). This dynamic must be well understood to interpret LAI from remotely sensed data.

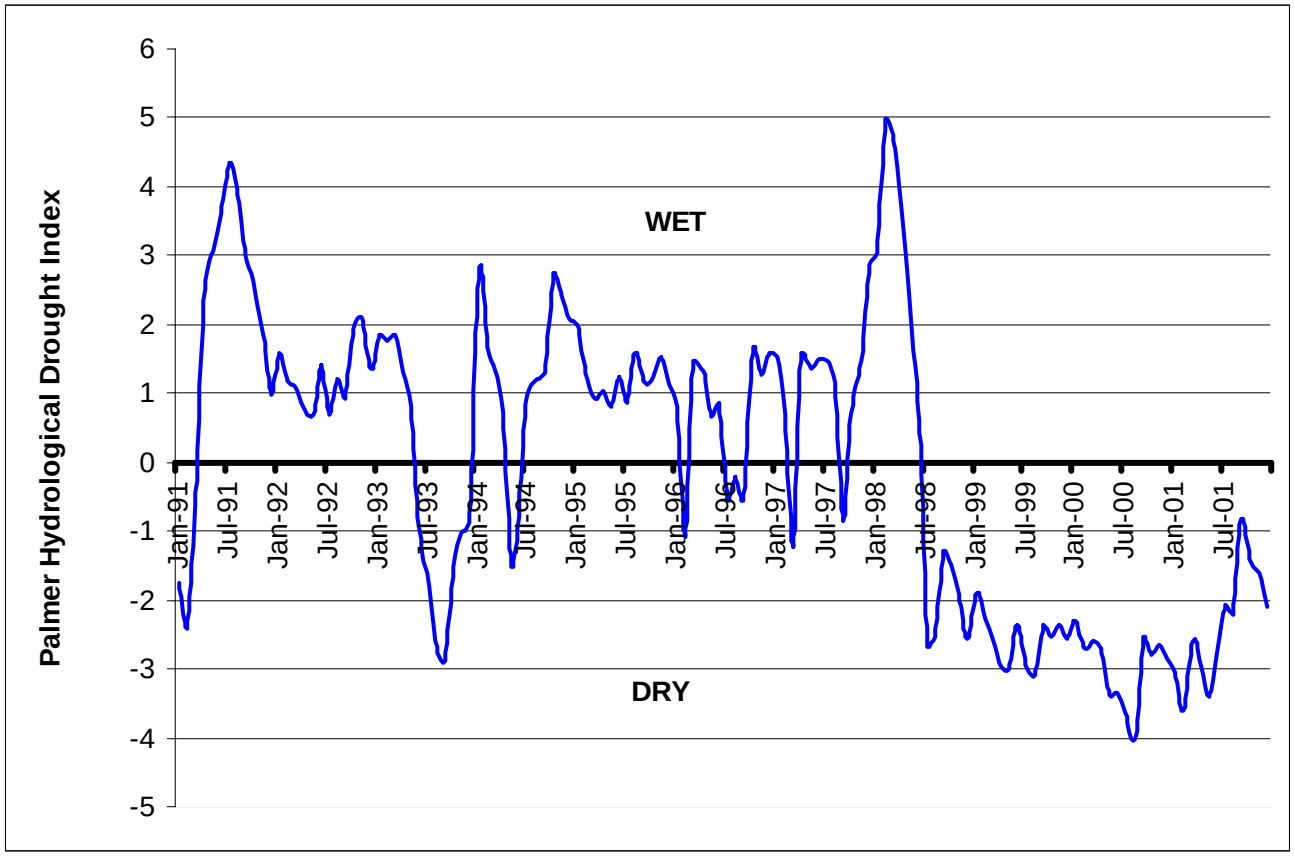

Figure 2-2. Characterization of north-central Florida climate during study period 1991-2001 (National Climatic Data Center 2005).

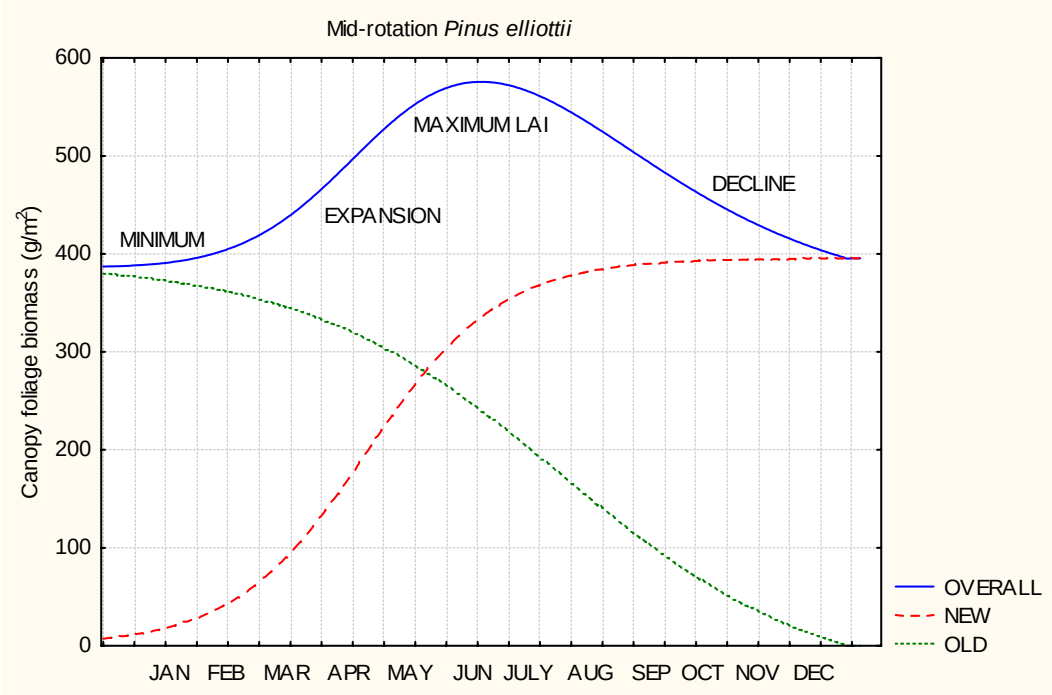

Figure 2-3. Annual cycle of variation in leaf phenology illustrating two populations of needles (Cropper and Gholz, 1993).

In situ estimates of LAI were calculated by leaf litterfall collection. Needlefall was collected monthly from six 0.7m² traps distributed randomly within each of the 24 IMPAC study plots from year 8 (1991) with the assumption of closed canopy through 2001. A similar method was used at the Donaldson site's four study plots, the results of which were aggregated into a single value for the tract.

LAI from litterfall was estimated using foliage accretion models (Martin & Jokela 2004). LAI results were presented as hemi-surface leaf area and converted to projected leaf area for integration with remote sensing data.

Integration of Ground Referenced LAI and Remote Sensing Data

LAI data based on monthly leaf litterfall collection from all 24 study plots was ground referenced to plot centroids based on GPS survey. Data from IMPAC ranged in date from January 1991 with the assumption of canopy closure at age 8 to February 2001,

the latest calculations available. Data from the Donaldson Tract ranged from April, 1999 with a similar assumption of canopy closure, to February 2001.

Landsat images were overlaid with plot locations within a geographic information system (GIS). Surface reflectance data and ground referenced LAI were related by a point method which joined LAI values to pixels based on the presence of a plot centroid. LAI data, aggregated monthly, were matched with image date based on proximity.

The integration resulted in a dataset based on the point method of 453 samples which linked 28 locations with their respective surface reflectance values at specific times over a period of 11 years. All rows were randomized within the table and 51 cases were extracted and withheld for external validation.

The data were densified with vegetative indices including normalized difference vegetative index (Birth, 1968), simple ratio (Rouse *et al.* 1973; Crist & Cicone 1984) and tasseled cap analysis components (Crist and Cicone 1984). Ancillary data were incorporated into the set including climate indexes and categorical plot data representing species type, plot treatment and phenological period. The complete list of variables used in modeling is included in Appendix A.

Climate variables

Local climatic conditions were represented by the Palmer Hydrological Drought Index (PHDI), a monthly index of the severity of dry and wet spells used to access long-term moisture supply (Karl & Knight 1985). The variety of indexes developed by Palmer and others standardize climatic indicators to allow for comparisons of drought and wetness at different times and locations. The PHDI was used instead of the better known rainfall-based Palmer Drought Severity Index (PDSI) because it accounts for site water balance, outflows and storage of water based on short-term trends.

The time scales at which climate influences leaf area are unknown. Therefore several variables were developed to explore specific lags: a simple annual lag, a summation of PHDI values during the leaf expansion period, that summation with an annual lag and finally a summation for PHDI during leaf expansion for current and previous growing years. This last variable is an attempt to capture the cumulative effect of climate when represented by two age classes of needles present during the maximum LAI period. Correct chronological sequence between phenology and climate indicators was maintained by interacting lagged variables with appropriate phenological periods.

Statistical analysis

Statistical analysis was performed on the integrated data set including descriptive, principle component and autocorrelation analysis using NCSS statistical software (Hintze 2001). The likelihood of spatial autocorrelation was explored using GEODA 0.9.5 geostatistical software (Anselin 2003).

Regression Techniques

Three types of regression processes were evaluated; two based on ordinary least squares (OLS), the third artificial neural networks (ANN).

Linear regression

Linear regression represents the simple form of OLS regression where a single independent variable, often a vegetative index, was regressed against the dependent variable LAI. Linear regression has been the typical approach in previous studies including Gholz and Curran (1991) using NDVI and Flores (2003) using SR.

Multivariate regression

In the multiple form of OLS regression, many independent variables, including surface reflectance data, vegetative indices, climate data and categorical data were

regressed against the dependent LAI. Stepwise variable selection was used to identify variables significant at p-value < 0.05.

Artificial neural network

Construction and processing of ANNs was accomplished with the neural network module of Statistica statistical software (StatSoft 2004). Architectures were limited to Multilayer Perceptron with a maximum of four hidden layers as suggested by Jensen *et al* (1999). A back-propagation training algorithm was used to train the network with a sigmoidal transfer function activating nodes. Sample sets were bootstrapped based on available cases. One hundred architectures were evaluated per model, with the top 5 retained based on the lowest ratio of standard deviation between residuals and observation data. From these five a 'best' model was selected based on the relationship between predicted and observed values from the training and validation set (r^2, RMSE).

Use of ancillary data to specify model sets

An advantage of multiple regressions (including ANN) over linear regression is the ability to include important locational information that is available but outside of the primary data source through the use of additional continuous or categorical variables. In particular the incorporation of categorical variables specifying phenological periods, species and treatments allow the relationship between LAI and its predictors to be generalized to a single model.

Three classes of multiple regression models are evaluated in this work: (1) simple models whose constituent variables are generated solely from remote sensing data and corresponding vegetation indices only; (2) intermediate models that additionally incorporate image date (and therefore phenological information) and climate data: (3) the most complex models that add stand level data such as species and treatment. Following

precedent set by Gholz and others the simple and intermediate models sets were developed for single species and single phenological periods.

Results

LAI values from leaf litterfall collection vary from just under 0.5 to 4.5 with a mean of 2.38 $m^2 m^{-2}$.There is considerable overlap in LAI for slash and loblolly (Figure 2-4.). There is a disproportionate effect of fertilization on species, with loblolly exhibiting an increase of 1.0 in mean LAI as compared to 0.56 for slash (Figure 2-5.).

One of the limitations of relating LAI to remote sensing data is spatial autocorrelation. Band 6, which detects emitted thermal radiation, exhibited significant spatial autocorrelation (Moran's I = 0.53) likely due to its coarse resolution of 120m (Landsat TM), an extent which overlays several plots at once. Spatial autocorrelation was not indicated for the reflectance values of the other 5 bands and LAI (Moran's I =0.03 and -0.02 respectively).

When two or more of the independent variables of a multiple regression are correlated, the data is said to exhibit multicollinearity. Multicollinearity may result in wide confidence intervals on regression coefficients. Principle component analysis of spectral variables used revealed eigenvalues near 0.0 for 5 of the 9 resultant components, indicating multiple collinearity. There was, however, little correlation between regional climate conditions, as indicated by the Palmer hydrological drought index and LAI for both species.

In general, the simplest possible predictive model is desirable. Simpler models are easier to apply to new cases because of the reduced requirements for input data. Complex environmental systems with multiple interacting biological and physical components are

however not likely to be adequately modeled by the simplest models. In this study we have examined a range of models from simple linear models through non-linear ANN multiple regression models. Our goal was to find a model that was a good predictor for separate validation data. The latter requirement was necessary as a guard against "overtraining" (Mehrotra *et al*. 2000).

Linear Models

For comparison purposes previously published models are listed above new models (Table 2-2). Of the 20 models tested 16 failed to reject the null hypothesis $\beta_1 = 0$. No model exceeded an $r^2 > 0.12$. These simple models were not adequate predictors of LAI for the training data. Even the published models with a history of useful predictors of southern pine LAI failed for this dataset.

Multiple Regression Models

All models tested statistically significant for slope representing improvement over linear models. r^2 values ranged from 0.31 to 0.70. In validation testing, increasingly complex models accounted for greater variation in LAI for training data, but performance with testing data was mixed. (Table 2-3). ANOVA analysis of significant variables appear in Table 2-5. Significant variables include presence or absence of fertilization treatments and phenological periods.

ANN Multiple Regression Models

The ANN predictions improved on OLS multiple regressions at each class strata. r^2 values ranged from 0.4 to 0.85 in training validation, and from 0.02 to 0.77 in testing (Table 2-4).

The generalized southern pine LAI predictive model (GSP-LAI) was selected as the top performing model (Figure 2-6). In validation tests the model explained > 75% of variance ($r^2 = 0.77$) with an RMSE < 0.50.

Discussion

In this study we created GSP-LAI, a model which effectively predicted LAI for a managed southern pine forests system of two species, multiple management treatments and climate variability on annual and seasonal scales. The model's development was guided by three major factors: 1) a focus on a relatively simple and well understood forest system for which there was ample data, 2) a desire to create an operational solution with wide applicability, and 3) the willingness to employ sophisticated regression techniques.

The intensively managed pine plantation is a simple system compared to natural regrowth forests or mixed coniferous/deciduous forests in terms of the presence of even-aged stands and the reduction of canopy layers (Gholz *et al*. 1991). Although seemingly an ideal system for LAI prediction, previously published southern pine LAI predictors applied to new remote sensing data lead to results so inaccurate as to be unusable as inputs for forest productivity modeling. New simple linear regression models constructed using single vegetative indices and trained on the study's large database offered no improvement.

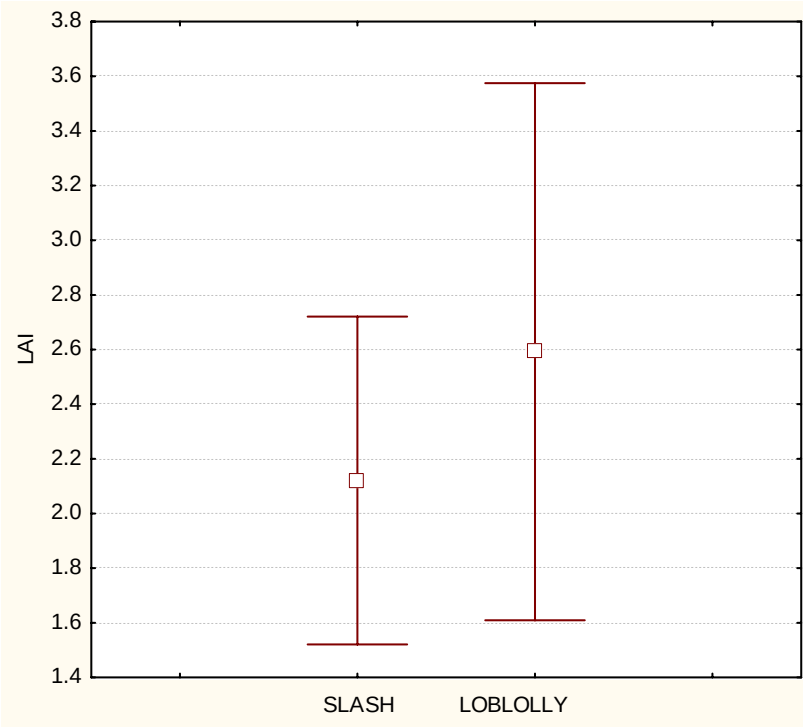

Figure 2-4. Comparison of the range of LAI values for slash and loblolly pine for all sites, 1991-2001.

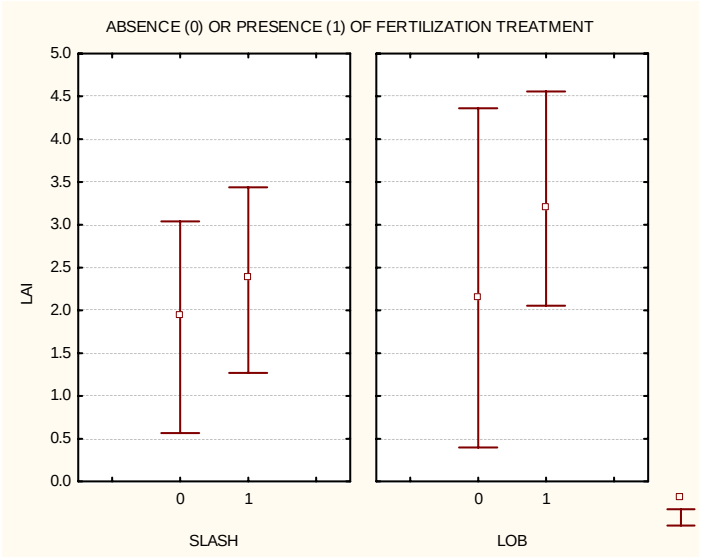

Figure 2-5. Differences in effect of fertilizer treatment on slash and loblolly pine.

Table 2-2. Summary of linear models fitted to dataset. First two models are previously published.

Model	Spp.	Phenological category	*n*	*a* Intercept	*b* Slope	r^2	RMSE	T Value	Prob. Level	Reject H0
Gholz (1991) † LAI = *a* + *b*(NDVI)	S	END	79	-14.31	32.25	0.03	1.50	20.80	<0.001	yes
		MAX	74	-20.02	43.62	<0.01	6.66	37.7	<0.001	yes
		MIN	36	-10.80	26.29	<0.01	3.59	-0.21	0.8344	no
Flores (2003) ‡ LAI = *a* + *b*(SR)	L	EXP/END	139	-0.83	0.56	0.01	1.75	0.25	0.2487	no
LAI = *a* + *b*(NDVI)	S	MIN	36	1.65	-0.15	<0.01	0.43	-0.2	0.9821	no
		EXP	20	3.76	-3.70	0.03	0.46	-0.72	0.4762	no
		MAX	73	2.54	-0.12	<0.01	0.59	-0.21	0.8356	no
		END	79	0.85	1.95	0.02	0.54	1.40	0.1652	no
	L	MIN	31	1.61	0.82	0.02	0.75	0.68	0.5018	no
		EXP	21	3.54	-1.57	<0.01	0.97	-0.15	0.8805	no
		MAX	68	2.95	0.49	<0.01	1.02	0.46	0.6468	no
		END	74	-0.60	6.05	0.12	0.80	3.20	0.0020	yes
LAI = *a* + *b*(SR)	S	MIN	36	1.67	-0.01	<0.01	0.43	-0.08	0.9353	no
		EXP	20	4.03	-0.75	0.03	0.46	-0.79	0.4308	no
		MAX	73	2.55	-0.3	<0.01	0.59	-0.21	0.8320	no
		END	79	1.15	0.22	0.02	0.54	1.18	0.2397	no
	L	MIN	31	1.53	0.17	0.02	0.75	0.69	0.4928	no
		EXP	21	3.58	-0.29	<0.01	0.97	-0.16	0.8779	no
		MAX	68	2.83	0.13	<0.01	1.02	0.62	0.5375	no
		END	74	-0.19	0.87	0.12	0.80	3.12	0.0025	yes

†Based on surface reflectance values ‡ Based on exoatmospheric reflectance values

Table 2-3. Summary of OLS multiple regression models fitted to dataset

Class	Label	Model†	Spp.	Phenological category	Validation					
					Training			Testing		
					n	r²	RMSE	*n*	r²	RMSE
Remote sensing data only	PASEND	LAI = -0.54+ 5.70E-02(B1)- 5.27E-02(B5)+ 8.08E-02(TCA-2)	S	END	79	0.31	0.459	13	0.51	0.37
	PALEND	LAI = -2.48 + 1.23(SR)+ 0.11(TCA-3)	L	END	74	0.33	0.707	8	0.05	1.05
Include Categorical and Climate Variables	PBSTOT	LAI = 2.35- 0.79(EXP) – 0.045(LAG-PHDI) – 0.63(MAX) – 0.40(MIN) – 6.32(NDVI) + 0.06(PHDI) + 1.20(SR) + 0.06(TCA-3)	S	ALL	208	0.42	0.497	27	0.02	1.40
	PBLTOT	LAI = 2.04 -1.03(EXP) - 0.74(MAX) -0.68(MIN) - 14.78(NDVI) + 3.02(SR)+ 0.09(TCA-3)	L	ALL	194	0.43	0.794	20	0.17	0.92
General Model	PCTOT	LAI = 4.48-1.038(EXP)- .902(FERT)-.508(HERB)- .835(MAX)-.515(SPP)+ 0.0308(TCA-3)	ALL	ALL	402	0.70	0.49	47	0.63	1.97

†B1= Band 1; B5= Band 5; TCA-2, 3= Tassel cap analysis component 2, 3; SR= Simple ratio vegetative index; MIN, EXP, MAX= phenological period: minimum LAI, expanding LAI, maximum LAI; PHDI= Palmer hydrological drought index; LAG-PHDI= PHDI one year previous; NDVI= Normalized difference vegetative index; FERT= Fertilization; HERB= Herbicide application; SPP= Species of tree. Details about variables are contained in Appendix A.

Table 2-4. Summary of ANN models fitted to dataset

Class	Label	Network architecture: Inputs	Hidden Layers	Nodes per Layer	Spp.	Phenological category	Validation: Training *n*†	Training r²	Training RMSE	Testing *n*	Testing r²	Testing RMSE
Remote Sensing data only	ASEND5	6	2	16, 12	S	END	79	0.40	0.422	26	0.02	1.10
	ALEND9	7	1	4	L	END	74	0.40	0.650	18	0.26	1.30
Include Categorical and Climate Variables	BSCLIM10	14	2	16, 6	S	ALL	213	0.42	0.490	27	0.39	0.52
	BLCLIM5	15	2	16, 7	L	ALL	190	0.49	0.784	24	0.12	0.94
General Model	GSP-LAI	18	2	16, 7	ALL	ALL	402	0.85	0.347	51	0.77	0.40

† Number of cases available for bootstrap sampling.

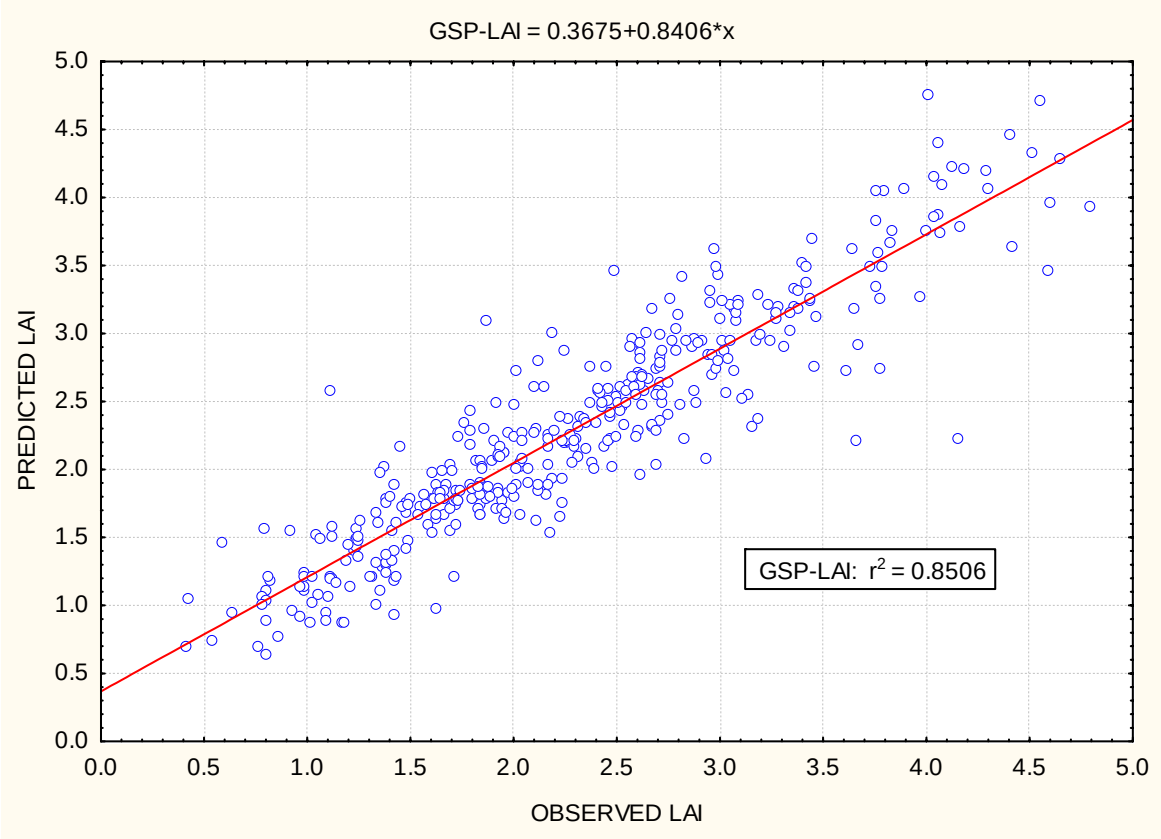

Figure 2-6. Plot of LAI values predicted by GSP-LAI for training data.

It is unclear if the previously published models were ever intended for use outside of the image from which they were created; they were developed with relatively few samples and with few sample dates. Climate history and leaf phenology would necessarily differ from remote sensing data used for model calibration. These shortcomings lead to a criterion that LAI estimation should not be limited to a single image, location, phenological period or satellite sensor. The poor performance of linear regression techniques applied to a robust dataset lead us to the conclusion that even this simple system was too complex to be predicted by a single variable.

In addition to the remote sensing data there are many variables that might be useful predictors of the system, including climate variables, management treatments such as fertilization, the presence and/or contribution of understory, phenological period, and others. To incorporate these variables multivariate regression techniques were necessary. The availability of ANN regression functions in modern statistical software allowed for the quick explorations of predictive networks to compare to OLS regressions.

In both OLS and ANN regression the highest performing models were the most general, capable of incorporating both continuous and categorical variables into a single solution. The assignment of categorical variables is a useful and underexploited technique permitting the development of models with wide domains of application.

OLS Multiple Regression Models

OLS regression revealed some of the probable drivers of this system, namely phenological period and management treatment. Tassel cap component 3 was the only consistent remote sensing variable used between models (Table 2-5). This component, also known as "wetness", is typically associated with evapotranspiration (ET) which is expected to increase with increased LAI. Tassel cap components are the product of coefficients for all 6 bands of reflected radiation that TM and ETM+ record and as such exploit more spectra than the commonly used NDVI and SR (Cohen *et al*. 2003).

ANN Models

The best general model was the product of ANN regression. This non-parametric technique was able to incorporate climate data as represented by PHDI and its lagged derivatives. Climate, while assumed to be important, is typically absent in the development of these sorts of empirical models. It is a difficult problem: eligible satellite images are all captured on sunny days, and the various temporal scales on which local

climate influences vegetation is mostly unknown and likely to be species and site specific. Typical data used in multitemporal analyses exhibit serial autocorrelation, necessitating transformations in order to become valid OLS inputs. The improved performance conveyed by the ANN regression suggests that 1) climatic variables are significant and 2) OLS regression was unable to use the variables as employed.

The GSP-LAI model is deterministic and easily implemented. Code for the model is detailed in Appendix B.

Fertilization

In the OLS and ANN generalized models fertilization represents a significant variable (Tables 2-5, 2-6). This result supports observations (Figure 2-5) and also Martin and Jokela's (2004) analysis of IMPAC leaf litterfall data. Fertilization is a focal treatment in intensive management practices, and indications of canopy response in the form of LAI assessment could direct the location and frequency of application. The availability of reliable LAI data could lead to a paradigm change in management practices were the goal becomes optimization of leaf growth based on site potential.

Suggestions for Future Effort

The improved performance of increasingly complex models provides insight into variables which drive or improve the predictability of LAI. Of these climate variables are particularly interesting in that they are widely assumed to play a role in canopy appearance and yet are rarely incorporated in empirical analysis. Difficulties exist in how to characterize climate, i.e. in terms of rainfall or temperature, and on what temporal scales it operates. Climate data necessarily suffers serial autocorrelation, a violation of assumptions required for OLS regression.

Table 2-5. ANOVA analysis of highly significant variables in OLS multiple regression. Other, less significant variables not shown.

Model	Variable	Df	r^2	Sum of Square	Mean Square	F-ratio	Prob. level	Power (5%)
PCTOT	FERT	1	0.22	69.48608	69.48608	286.143	<0.0001	1
	MAX	1	0.1612	50.91658	50.91658	209.674	<0.0001	1
	EXP	1	0.1053	33.25625	33.25625	136.949	<0.0001	1
PBSTOT	MAX	1	0.149	12.7119	12.7119	51.476	<0.0001	1
	TCA-3	1	0.0902	7.697152	7.697152	31.169	<0.0001	0.9998
PBLTOT	TCA-3	1	0.1572	32.37256	32.37256	51.311	<0.0001	1
	MAX	1	0.0818	16.85336	16.85336	26.713	<0.0001	0.9993
PASEND	TCA-2	1	0.2165	4.925346	4.925346	23.39	<0.0001	0.9976
PALEND	SR	1	0.2191	11.53746	11.53746	23.087	<0.0001	0.9973
	TCA-3	1	0.2065	10.87232	10.87232	21.756	<0.0001	0.9959
	B1	1	0.1444	3.284696	3.284696	15.599	0.0002	0.9737

Sensitivity analysis of the GSP-LAI model indicates that a non-parametric, non-linear technique can make use of that data at various lags, a tantalizing clue which should inspire additional research (Table 2-6).

Table 2-6. Sensitivity analysis of variables used in ANN multiple regressions.

	Model Label				
Rank	**ASEND**	**ALEND**	**BSCLIM**	**BLCLIM**	**GSP-LAI**
1	TCA-1	B2	B1	END	END
2	B5	TCA-3	B4	MAX	FERT
3	B4	TCA-1	EXP-PHDI	B7	B2
4	B2	SR	TCA-3	LAG1-PHDI	B5
5	TCA-2	TCA-2	SUM-EXP-PHDI	B1	SPP
6	B1	B4	B5	NDVI	HERB
7		B1	MIN	MIN	PHDI
8			EXP	B3	TCA-1
9			LAG-PHDI	SR	MIN
10			TCA-2	PHDI	B3
11			SR	EXP-PHDI	EXP
12			B7	TCA-3	EXP-PHDI
13			PHDI	B2	SUM-EXP-PHDI
14			B2	TCA-2	LAG1-PHDI
15				B4	B7
16					LAG-PHDI
17					TCA-2
18					TCA-3

Variable codes appear in Appendix A.

The effectiveness of LAI predictions would be enhanced with a reduction of time between the acquisition of remote sensing data and its analysis. The use of ground referenced LAI from litterfall necessitates an 18 month lag in processing from collection to value. Using optical methods to indirectly measure LAI *in situ* would likely reduce this lag provided corrections as suggested by Gower *et al* (1999) were incorporated to maintain accuracy.

With minor modification the GSP-LAI model can be adapted to new remote sensor that share 'legacy' characteristics with TM and ETM+. Due to mechanical malfunctions

the ETM+ sensor has become an unreliable source of remote sensing data. Data captured by the Advanced Spaceborne Thermal Emission and Reflection Radiometer (ASTER) is particularly interesting for this application. Aboard the TERRA platform, ASTER flies the same orbit as Landsat and shares similar spectral, radiometric and temporal resolution as ETM+ with recording at additional bandwidths. Integrating ASTER data into GSP-LAI would allow for continuous analysis into the reasonable future.

The substantial LAI data collected by the researchers at IMPAC and other sites should be maintained and expanded if possible. These sites should be oriented to Landsat legacy coordinates, and a minimum size is recommended at 1.5 times the 30 m pixel resolution, which would allow for the ±0.5 pixel georectification error. Designed in this fashion sites could serve to train and 'calibrate' existing and future LAI predicting models.

Conclusions

The development of empirical models relating ground-referenced parameters to remote sensing data may be greatly facilitated using multivariate regression techniques. The specification of ancillary variables are an effective way to include the unique biology of a given system, in this study represented by seasonal leaf dynamics, variation in local climate and influential management practices. The use of these local variables was essential for developing a model which met the objectives of multitemporal and spatial applicability.

The evaluation of increasingly complex regression models was designed to expose simple solutions to the problem of LAI prediction if they existed. In this study none were found, and instead advanced non-linear techniques were required to incorporate

important data with non-normal distributions and multicollinearity such as serially correlated climate data.

CHAPTER 3
REMOTE SENSING AND SIMULATION TO ESTIMATE FOREST PRODUCTIVITY IN SOUTHERN PINE PLANTATIONS

Introduction

Pine plantations of the Southeastern United States constitute one-half of the world's industrial forests and account for 60% of the timber products used in the United States (Prestemon & Abt 2002). In Florida alone industrial timber is the leading agricultural sector, generating $16.6 billion in revenues in 2003 (Hodges *et al*. 2005). Almost half the State's land area is in forests concentrated in northern and central counties where this study is centered.

Managing these forests for maximum yield is a primary economic goal of timber interests; the rate at which these forests remove and sequester atmospheric carbon as woody biomass is of interest to climate change researchers who recognize forests as the only significant human-influenced sink of greenhouse gases (Tans & White 1998). Sequestered carbon is likely to become another revenue source as the global community endeavors to limit CO_2 emissions through cap-and-trade carbon exchange schemes such as those outlined by the Kyoto Protocol of 1997.

The net ecosystem exchange of carbon (NEE) in a landscape may be estimated through simulation given the system is somewhat homogenous, well understood and important biophysical parameters are known (Turner *et al.* 2004b). The SPM-2 model (Cropper & Gholz 1993; Cropper 2000) estimates NEE for slash pine (*Pinus elliottii*) plantations, a dominant plantation type in Florida and the subject of several studies

(Gholz *et al.* 1991; Teskey *et al.* 1994; Clark *et al.* 2001; Martin & Jokela 2004). SPM-2 simulates hourly fluxes of CO_2 and water, and accounts for the contributions of typical understory components including saw palmetto (*Serenoa repens*), gallberry (*Ilex galabra*) and wax myrtle (*Myrica cerifera*). Annual estimates of net ecosystem carbon exchange simulated by SPM-2 matched measured values from an eddy covariance flux tower site (Clark *et al.* 2001).

Although SPM-2 was originally designed to simulate individual stand dynamics it may be scaled to broad biogeographical extents with inputs of spatially referenced leaf area index (LAI) and stand age. LAI is the ratio of leaf surface supported by a plant to its corresponding horizontal projection on the ground; as such LAI has direct correspondence with the ability of the canopy to absorb light to conduct photosynthesis (Asner & Wessman 1997).

LAI's contribution as a primary biophysical parameter in NEE simulation also makes it an important indicator of productivity for land managers. Current silvicultural practices focus on improving the availability of resources, through fertilization and herbicidal control of understory, to increase stem growth. Sampson *et al* (1998) suggest management for increased leaf growth could introduce efficiencies related to site growth potential that would otherwise be missed.

LAI is difficult and expensive to assess *in situ* resulting in sparse sample sets that are necessarily localized at a stand scale and thus difficult to extrapolate to larger extents (Fassnacht *et al*. 1997). A model which determined LAI from remotely sensed data would have the advantage of being spatially explicit, scaleable from stand to regional or larger extents, and would sample remote or inaccessible areas (Running *et al*. 1986). An

ideal empirical model linking ground-referenced LAI to remote sensing data would be make reliable predictions at various extents and image dates and be general enough to incorporate important local information such as climatological and phenological data.

The generalized southern pine LAI predictive model (GSP-LAI) described in Chapter 2 satisfies many of these criteria in that it uses Landsat Thematic Mapper (TM) and Enhanced Thematic Mapper Plus (ETM+) imagery to make high resolution (30 m) estimates of LAI for slash and loblolly plantations captured within the image's 185 km wide swath. Climate variables are incorporated in the form of Palmer's Hydrological Drought Index (Karl & Knight 1985) at image date and in various lags; categorical variables representing phenological period and stand data such as age and silvicultural treatments are also included.

With the input of spatially explicit LAI values NEE may also be simulated for the same extent and resolution. Previous studies have estimated components of NEE with coupled remote sensing and simulation model approaches for diverse forest stands with multiple dominant species (Lucas *et al.* 2000; Smith *et al.* 2002; Turner *et al.* 2004a). The GSP-LAI model was developed for loblolly and slash pine plantations and the SPM-2 models is limited to closed-canopy slash pine forests (age 8 or older). Slash pine plantations are an important forest type in northern Florida, and the simple forest ecosystem provides the potential for greater precision and for outputs relevant to commercial forestry.

Objectives. In this study we apply the GSP-LAI model to a Landsat ETM+ image of an extensive pine plantation holding in North-Central Florida and estimate 1) Leaf Area Index and 2) NEE based on integration with the SPM-2 model.

Methods

Spatially explicit LAI values were estimated for the plantation pine within the study extent using the GSP-LAI model and brightness values recorded by the Landsat 7 Enhanced Thematic Mapper Plus sensor on September 17, 2001. LAI values and stand age were used to generate estimates of NEE using the slash pine specific forest productivity model SPM-2.

Study Area

The study extent is comprised of a 178,655 ha (441,467 acre) landscape centered at 29° 51.5´ N, 82° 10.7´W near Waldo, Florida USA (Figure 3-1). This extent contains many classes of land cover/ land use including open water, urban and agricultural. Of specific interest are 11,142 ha (27,520 acres) of intensively managed slash and loblolly plantation forests which as of image date were closed canopy (8 years old or older). Of this 83% was planted in slash and 17% loblolly pine. Other classes of forest were excluded from analysis including natural regrowth areas, recently cut or planted stands, and stands which contained other species of pine, such as longleaf pine (*Pinus palustris*), or hardwoods.

Stand data was provided by Rayonier, Inc. and indicated date of establishment, planting density and silvicultural treatments, including date of fertilization or herbicide application.

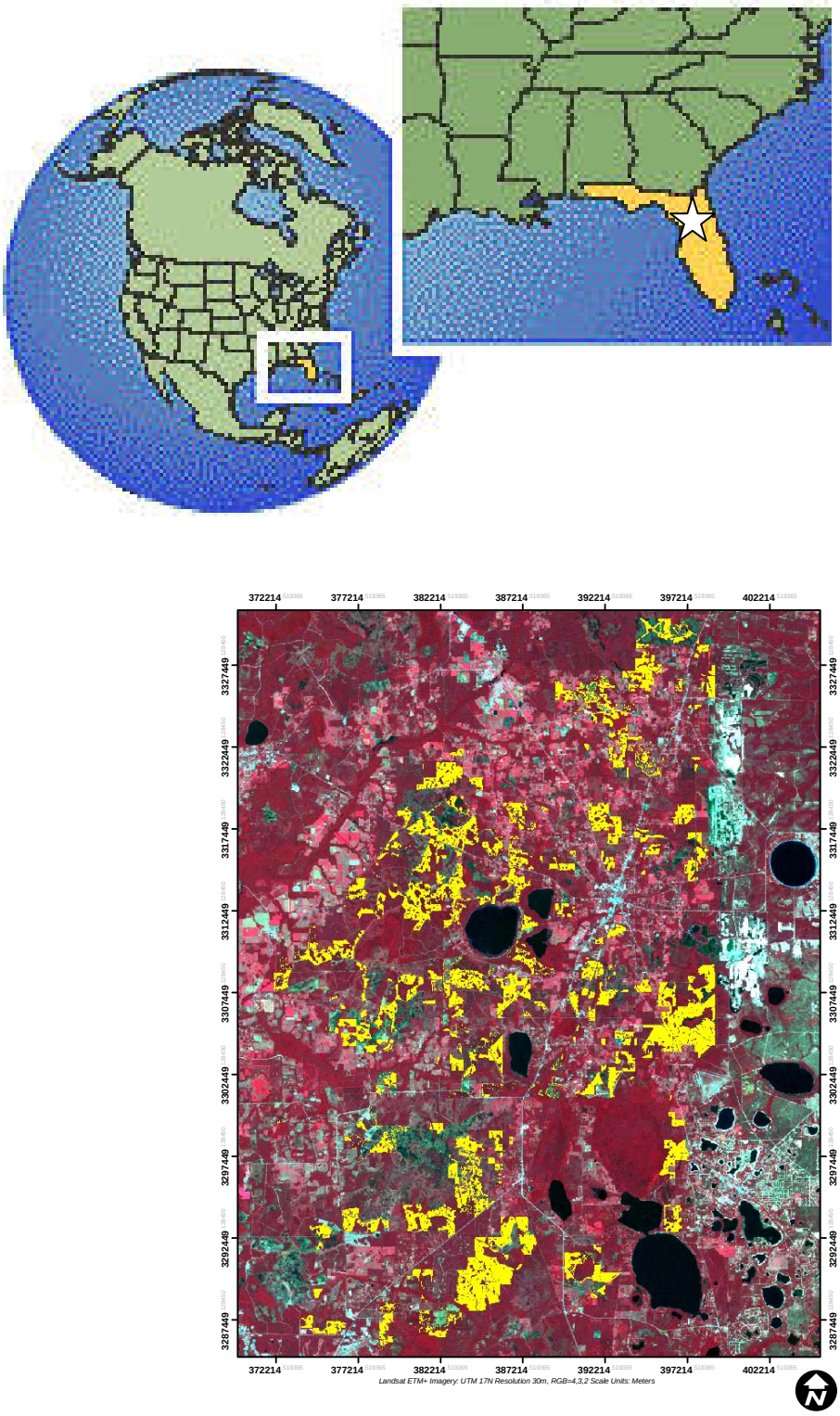

Figure 3-1. Map of the Bradford Forest, Florida, USA. Yellow indicates forest extent; background is a false color mosaic from Landsat ETM+.

Integration of Remote Sensing and Ground Referenced Data

The study extent was imaged by Landsat 7 Enhanced Thematic Mapper Plus (ETM+) on September 17, 2001 at approximately 11:00 am on a cloudless day. The image was geographically rectified using a second order polynomial equation with between 30 and 40 ground control points. Rectification error reported as < ±0.5 pixels.

Vector-based stand data was converted to raster format and matched to remote sensing data in an overlay procedure within image processing software (Leica Geosystems GIS and Mapping 2003). Ancillary information such as climatic and phenological data was incorporated in the same manner. The resultant layer stack was reported as a text file with over 150,000 rows of pixel information including coordinates and imported into a Statistica spreadsheet (StatSoft 2004) where it was densified with tassel cap components 1-3 (Huang *et al*. 2002).

Processing Data with the GSP-LAI and SPM-2 Models

The GSP-LAI model was employed within the Statistica neural network interface. Resultant LAI values were reported in spreadsheet format and made ready for SPM-2 by 1) masking of non-forest pixel anomalies comprised of negative LAI values, and 2) extraction of slash-only values.

Processing of LAI values and stand age resulted in an estimate of NEE in Mg ha^{-1} yr^{-1} for each pixel defined by coordinates. Both NEE and LAI results were imported into a geographic information system (ESRI 2003) and projected as a map.

Results

The GSP-LAI model estimated LAI for 10,797 ha (26,700 acres) of slash and loblolly pine plantations. Values ranged from 0 to 3.93 with a mean of 1.06 (Figure 3-1).

Approximately 1% of the area analyzed exhibited very low LAI values (< 0.1) which were associated with forest edges.

The SPM-2 model estimated NEE for plantation slash pine totaling 9,770 ha (24,131 acres). Values ranged from -5.52 to 11.06 Mg ha^{-1} yr^{-1} with a mean of 3.47 Mg ha^{-1} yr^{-1} (Figure 3-2). As with the LAI values very low NEE was exhibited at forest edges. Approximately 1.6% of the area analyzed exhibited NEE values greater than 8.0 Mg ha^{-1} yr^{-1}, a maximum value reported by Starr *et al* (2003) from a Florida Ameriflux study of slash pine in north-central Florida. Total carbon balance for the area analyzed is 33,920 metric tons representing 87,243 tons of CO_2 or about 9 tons per acre.

By means of associated map coordinates these values were categorized and displayed on a map along with the Landsat image used as the primary data source (Figure 3-3, 3-4).

Discussion

The feasibility of estimating forest productivity in terms of NEE was demonstrated using empirical and simulation models based on remotely sensed data. Despite our inability to ground-truth the resultant values for LAI and NEE are plausible and in the realm of expected values. The utility of these estimates is enhanced by their landscape scale and that carbon gain and loss are attributed to specific stands and ownership. These results offer proof of concept and further work is encouraged.

Based on the May 27, 2005 price of $1.30 per 100 T CO_2 the estimated value of carbon sequestered in this analysis is $102,891.10 or $4.26 per acre (Chicago Climate Exchange 2005).

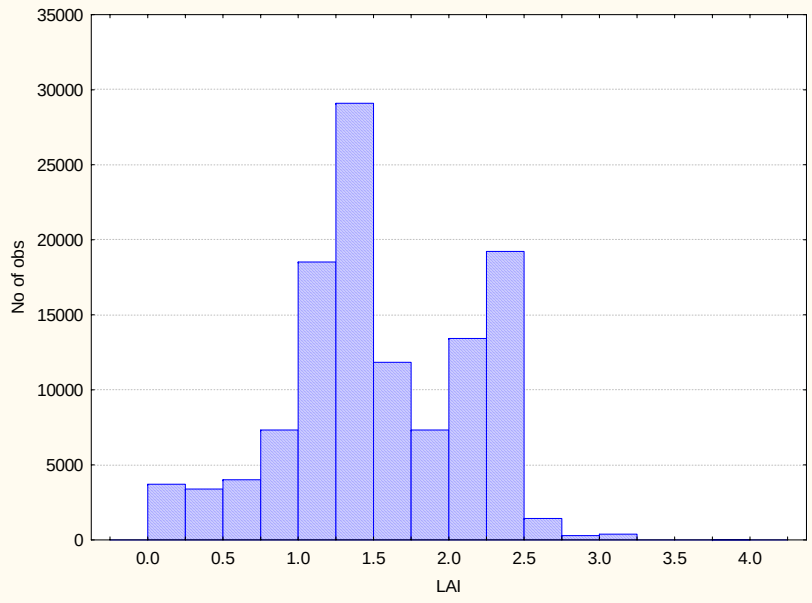

Figure 3-1. Predicted LAI values for closed canopy slash and loblolly pine. Bradford FL

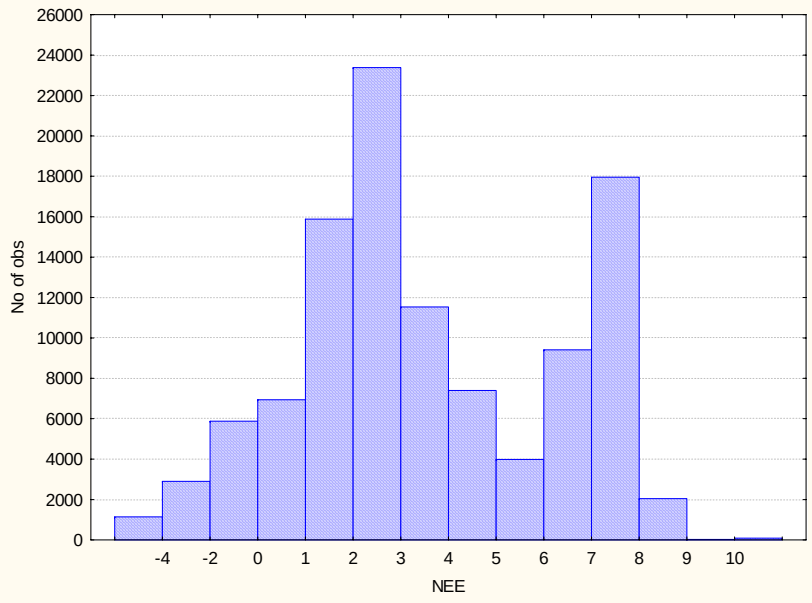

Figure 3-2. Predicted NEE values for closed canopy slash and loblolly pine. Bradford FL

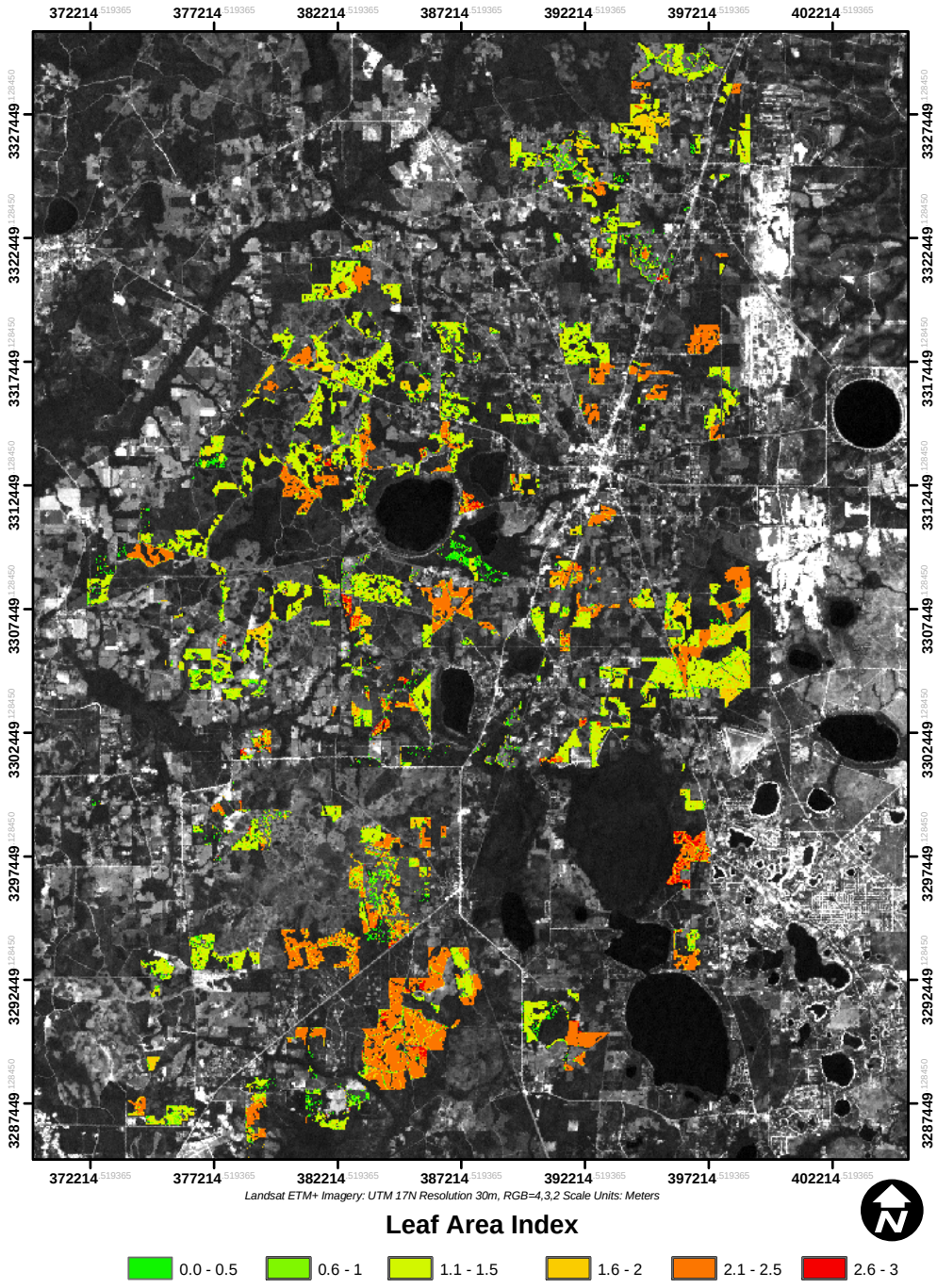

Figure 3-3. Predicted LAI values for southern pine plantations in north-central Florida for September 17, 2001

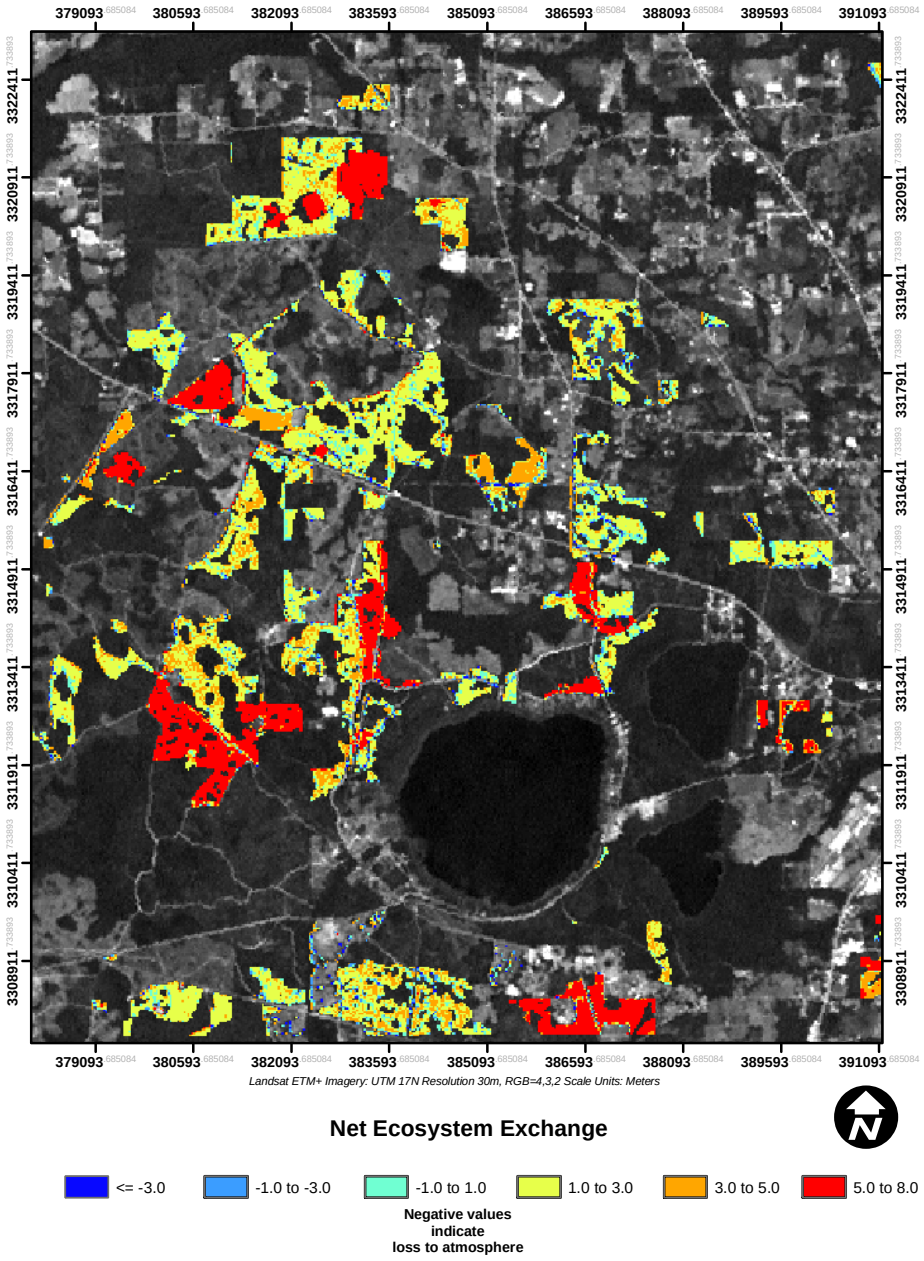

Figure 3-4. Predicted NEE values for southern pine plantations in north-central Florida for September 17, 2001.

Visual analysis of the map (Figure 3-4.) reveals low LAI and NEE values along logging roads and for other mixed pixels representing partial contributions of forest. These values were not masked as they represent valid data and offer some confidence that the models are selective and appropriate.

The bimodal distribution of LAI values in Figure 3-1 can be traced to the effect of the variable fertilizer on the model (Figure 3-3). Fertilization is known to increase LAI in slash and loblolly (Martin & Jokela 2004); however ground truthing is needed to assess how close model predictions are to observations. Fertilization is a focal treatment in intensive management practices, and indications of canopy response could lead to efficiencies in the location and frequency of application. The availability of reliable LAI data could lead to a paradigm change in management practices were the goal becomes optimization of leaf growth based on site potential.

The conceptual framework presented here represents one way by which carbon sequestration may be monitored and inventoried, providing necessary underpinning for carbon trading schemes. Landscape-scale valuations of carbon sinks could lead to a revaluation of ecosystem services as nations acknowledge the benefits of removing greenhouse gases from the atmosphere.

Conclusions

This work provides a conceptual model whereby forest productivity may be estimated for a forest system using an empirically derived LAI prediction model and a process simulation model. Spatially explicit results of LAI and NEE values relate important forest attributes to specific ownership creating new opportunities for improved management.

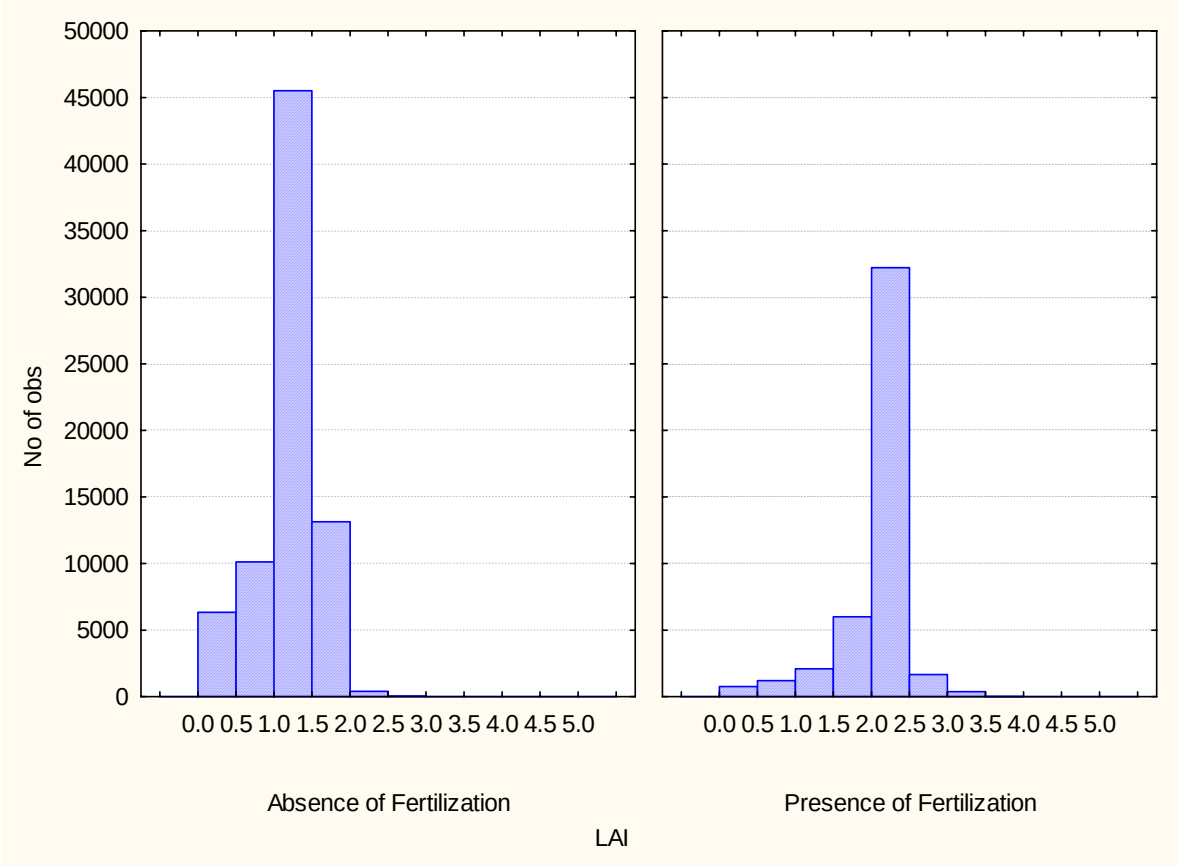

Figure 3-5. Effect of variable FERT on LAI prediction.

CHAPTER 4
SYNTHESIS

Results and Conclusions

In this study we developed an LAI prediction model which was novel in many respects: it used an advance regression technique to establish a non-linear relationship between the dependent and independent variables; the independent variables included important local information, an example being climate data, which is a widely recognized yet seldom employed driver of all things vegetative; models underwent a validation process. The GSP-LAI model represents an improvement over previous efforts in our study system.

The requirement of stand data by GSP-LAI may be criticized researchers desirous of LAI determination without *a priori* knowledge. The stratified model methodology illustrated that only tenuous relationships were established with remote sensing data only; furthermore significant explanatory improvements ($r^2 > 0.1$) are realized simply through the incorporation of basic phenology as indicated by image date.

The visualization of net ecosystem exchange of carbon via a map represents an advance in our management of slash pine carbon sequestration. It is noteworthy that these carbon totals are linked to specific ownership. It is foreseeable that industry rather than academia will advance carbon sequestration research once the perceived values of forest properties adjust to these new appraisals.

Pragmatically the availability of timely LAI data might influence a paradigm shift among forest managers away from current goals emphasizing resource availability

through fertilization and herbicide application, to an integrated approach that considers canopy response to treatments in the context of site potential and biological potential. Management approaches of this type are likely to improve yield while decreasing expense and impact on the environment.

Further Study

The substantial LAI data collected by the IMPAC and other sites should be maintained and expanded if possible. These sites should be oriented to Landsat legacy coordinates, and a minimum size is recommended at 1.5 times the 30 m pixel resolution, which would allow for the ±0.5 pixel georectification error. Designed in this fashion sites could serve to train and 'calibrate' existing and future LAI predicting models.

As technology advances higher quality remote sensing data is becoming available. Data from the Advanced Spaceborne Thermal Emission and Reflection Radiometer (ASTER) sensor integrates well with Landsat legacy operations yet offers an additional 7 bandwidths for analysis. Physical tree structure below the canopy is being recorded with light detecting and ranging (LIDAR) sensors. Many of the techniques presented in this study are able to integrate data from disparate sources.

APPENDIX A
VARIABLES USED IN MODELS

Variable	Tag	Type	Equation/ Bandwidth	Range	Notes
Band 1	B1	Continuous	0.45 – 0.52µm Blue	0 – 255	Surface reflectance, 8-byte
Band 2	B2	Continuous	0.52 – 0.60µm Green	0 – 255	″ ″
Band 3	B3	Continuous	0.60 – 0.63µm Red	0 – 255	″ ″
Band 4	B4	Continuous	0.69 – 0.76µm Near infrared	0 – 255	″ ″
Band 5	B5	Continuous	1.55 – 1.75µm Mid infrared	0 – 255	″ ″
Band 6	B6	Continuous	10.5 – 12.5µm Emitted thermal	0 – 255	Variable not used due to severe spatial autocorrelation
Band 7	B7	Continuous	2.08 – 2.35µm Mid infrared	0 – 255	Surface reflectance, 8-byte
Normalized Difference Vegetative Index	NDVI	Continuous	(B4 – B3)/(B4 + B3)	-1.0 – 1.0	Vegetation index
Simple Ratio	SR	Continuous	B4/B3	0 – 255	Vegetation index
Tasseled Cap Analysis Component 1	TCA-1	Continuous	0.2043(B1) + 0.4158(B2) + 0.5524(B3) + 0.5741(B4) + 0.3124(B5) + 0.2303(B7)		n-space vegetation index: “Brightness”
Tasseled Cap Analysis Component 2	TCA-2	Continuous	(-0.1603(B1)) + (-0.2819(B2)) + (-0.4934(B3)) + 0.7940(B4) + 0.0002(B5) + (-0.1446(B7))		n-space vegetation index: “Greenness”
Tasseled Cap Analysis Component 3	TCA-3	Continuous	0.0315(B1) + 0.2021(B2) + 0.3102(B3) + 0.1594(B4) + (-0.6806(B5)) + (-0.6109(B7))		n-space vegetation index: “Wetness”
Species	SPP	Categorical	Loblolly = 1 Slash = 0	N/A	Type of tree
Fertilizer	FERT	Categorical	Fertilized = 1 Not Fertilized = 0	N/A	Based on previous season
Herbicide	HERB	Categorical	Treated = 1 Untreated = 0	N/A	Maintained understory control

Minimum LAI period	MIN	Categorical	Within Minimum = 1 Other periods = 0	N/A	Minimum leaf biomass; spans ≈ March through April in region
Expanding LAI period	EXP	Categorical	Within Expansion = 1 Other periods = 0	N/A	Increasing leaf biomass; spans ≈ May through June in region
Maximum LAI period	MAX	Categorical	Within Maximum = 1 Other periods = 0	N/A	Maximum leaf biomass; spans ≈ July through September
Declining LAI period	END	Categorical	Within needlefall = 1 Other periods = 0	N/A	Minimum leaf biomass; spans ≈ October through February in study area. Implicit in multiple regressions
Palmer Hydrological Drought Index	PHDI	Continuous	Values generated by NOAA	-7.0 – 7.0	Monthly: indicates severity of dry and wet spells; dry negative values, wet positive values, norms ≈ zero
One year lag PHDI	LAG_PHDI	Continuous	Monthly PHDI – 1 year	-7.0 – 7.0	Previous year's PHDI
Expansion period PHDI	EXP_PHDI	Continuous Interactive	Average PHDI for March, April, May	-21.0 – 21.0	PHDI during leaf expansion; interacts with phenological period.
Previous season expansion period PHDI	LAG1_PHDI	Continuous Interactive	Lagged Average PHDI for March, April, May	-21.0 – 21.0	PHDI during leaf expansion; interacts with phenological period.
Two consecutive years expansion period PHDI	SUM_PHDI	Continuous Interactive	Sum Lagged Average PHDI for March, April, May	-42.0 – 42.0	PHDI during leaf expansion; interacts with phenological period.

APPENDIX B
GSP-LAI CODE

Note: this code written in python.

```
from Numeric import *
import math


class Predict_LAI:

   '" prediction of LAI by Artifical Neural Network model
   GSP-LAI model is 18:16:7:1 18 inputs, 2 hidden layers and 1 output
   Doug Shoemaker and Wendell Cropper  June, 2005"'


   def __init__(self):



      self.pattern = [25.0, 24.0, 48.0, 14.0, 101.1557, 9.9365,
                  4.0215, -0.63, -1.25, -4.94, -4.94,
                  -4.94, 0, 1, 1, 1, 0, 0]

      self.in_labels = ['B2 ','B3 ','B5 ','B7 ','TCA1 ','TCA2 ','TCA3 ','PHDI ','LAG_PHDI',
'EXP_PHDI','LAG1_PHDI','SUM_EXP_PHDI','SPP','FERT','HERB','MIN_LAI ',
'EXP_LAI ', 'END ']


      self.N_hidden = [16, 7] #number of nodes in each hidden layer; in order
                  # e.g., [4, 6, 9] for three layers
      self.N_input = 18

      self.N_layers = 2  # number of hidden layers

      self.afunc = [self.activ, self.activ] # each layer may have a separate activation
function
                        # [self.activ, self.activ, self.a2] for example


      self.W = zeros((self.N_input + 1, self.N_hidden[0]), Float32)
```

```
self.W2 = zeros((self.N_hidden[0] + 1, self.N_hidden[1]), Float32)
self.WO = zeros((self.N_hidden[1] + 1), Float32)

#weights from input to hidden

self.W[0][0] = -0.68070867581967331; self.W[1][0] = -0.47077273479909026
self.W[2][0] = -0.85230477952479411; self.W[3][0] = 0.33897992017428513
self.W[4][0] = 0.27701895076167499; self.W[5][0] = -1.0572088503393293
self.W[6][0] = 0.36528134122444544; self.W[7][0] = -0.99617510476443649
self.W[8][0] = -0.50428492164536609; self.W[9][0] = -0.18280550315894767
self.W[10][0] = -0.94167697838932418; self.W[11][0] = 0.98202982430634478
self.W[12][0] = 0.61440222032592962; self.W[13][0] = 1.1844340063249028
self.W[14][0] = -0.25002768723088353; self.W[15][0] = 0.63030042820138565
self.W[16][0] = 0.51299032922949417; self.W[17][0] = 0.44325306956489968
self.W[18][0] = 0.2248803488147274   #bias weight input should be 1.0

# NOTE: the bias (Threshold weight signs have been reversed (* -1)
# from the Statistica program c code to match the algorithm in SNNCode.cc

self.W[0][1] = 0.51346930771036581; self.W[1][1] = -0.82554800347023094
self.W[2][1] = 0.90426603023396934; self.W[3][1] = 0.58889085506156402
self.W[4][1] = -0.95958368729266708; self.W[5][1] = -0.90469199829822045
self.W[6][1] = -0.14307625257737089; self.W[7][1] = -0.20554967720687164
self.W[8][1] = -0.21554929367886586; self.W[9][1] = -0.34579555496400843
self.W[10][1] = 0.83046571076512765; self.W[11][1] = 0.32340290066403304
self.W[12][1] = -0.18118559428067804; self.W[13][1] = -0.75238704258583811
self.W[14][1] = -0.37747431711820228; self.W[15][1] = 0.85923511162687338
self.W[16][1] = 0.39065411751788415; self.W[17][1] = -0.20355515889674639
self.W[18][1] = 1.0246810022363515   #bias weight input should be 1.0

self.W[0][2] = -0.35311763505484994; self.W[1][2] = -0.4386456022349271
self.W[2][2] = -0.87637948900026352; self.W[3][2] = -0.72428696217924937
self.W[4][2] = -0.31671942062831882; self.W[5][2] = 0.05527068372351699
self.W[6][2] = 0.56535409825860228; self.W[7][2] = 0.51021420192585065
self.W[8][2] = 0.016770303367016015; self.W[9][2] = 0.34584426212393066
self.W[10][2] = -0.2487170315158326; self.W[11][2] = -0.10550485203992196
self.W[12][2] = -0.48798944879736178; self.W[13][2] = -0.6190887070661879
self.W[14][2] = -0.22993121833505939; self.W[15][2] = 0.50627708251063963
self.W[16][2] = -1.0785292527624635; self.W[17][2] = 0.033937996367607123
self.W[18][2] = 0.65202105499593555   #bias weight input should be 1.0

self.W[0][3] = -1.0409218053604059; self.W[1][3] = -1.0248054352063849
self.W[2][3] = 0.33260785739356169; self.W[3][3] = -0.26650614694911684
self.W[4][3] = -0.64306159332498813; self.W[5][3] = -0.59743303482074173
self.W[6][3] = -0.78619166931548001; self.W[7][3] = 0.45658535946357542
self.W[8][3] = -0.30551820237080174; self.W[9][3] = 0.99383562833852823
```

self.W[10][3] = 0.58314990180960924; self.W[11][3] = 0.37535417400887111
self.W[12][3] = -0.28530757703577508; self.W[13][3] = -0.090269033578186067
self.W[14][3] = 0.064328952896598818; self.W[15][3] = 0.97787174712308034
self.W[16][3] = 0.19248517688726832; self.W[17][3] = 0.33429026289740676
self.W[18][3] = -0.035729304447247368 #bias weight input should be 1.0

self.W[0][4] = -0.69171961247455427; self.W[1][4] = -0.19318811287043236
self.W[2][4] = -0.24535334151780164; self.W[3][4] = 0.83124440482653728
self.W[4][4] = -0.25125881212500051; self.W[5][4] = 0.67654822161911254
self.W[6][4] = 1.1935093304341891; self.W[7][4] = -0.1061578514825464
self.W[8][4] = 0.97769969375119914; self.W[9][4] = -0.62531219673983507
self.W[10][4] = 0.44887478855493629; self.W[11][4] = 0.25089122271948444
self.W[12][4] = 0.39739937692561506; self.W[13][4] = -0.11329258567683172
self.W[14][4] = -0.58529954873398038; self.W[15][4] = 1.0085035066605659
self.W[16][4] = 0.16742174428496126; self.W[17][4] = 0.58995422198121061
self.W[18][4] = 0.3348083808274705 #bias weight input should be 1.0

self.W[0][5] = -0.77429576139488687; self.W[1][5] = -0.15475931985401509
self.W[2][5] = 0.73579372223419681; self.W[3][5] = 0.1381863709121455
self.W[4][5] = 0.6873206129011652; self.W[5][5] = 0.46745295715611929
self.W[6][5] = 0.41009374571990187; self.W[7][5] = -0.87188230719585069
self.W[8][5] = -0.72335484095791835; self.W[9][5] = -0.91529433041239316
self.W[10][5] = -0.58370952581324753; self.W[11][5] = -0.67397946658272845
self.W[12][5] = -0.34210837715877956; self.W[13][5] = -0.41773337644458219
self.W[14][5] = 0.47038952274991436; self.W[15][5] = 0.093448267923307141
self.W[16][5] = 0.26835793839884453; self.W[17][5] = 0.22325046302604781
self.W[18][5] = -1.0210341534849725 #bias weight input should be 1.0

self.W[0][6] = 0.080858496314387546; self.W[1][6] = 0.0084803147734866177
self.W[2][6] = -0.45972948915316991; self.W[3][6] = -1.0221823283337763
self.W[4][6] = -0.011916970527570785; self.W[5][6] = 0.2898749572896876
self.W[6][6] = -0.70301410605914416; self.W[7][6] = -0.96795643773447171
self.W[8][6] = 0.19725907114720687; self.W[9][6] = 0.20975438358448029
self.W[10][6] = 0.36924810928999657; self.W[11][6] = -0.10139479969175098
self.W[12][6] = -0.060662670497412904; self.W[13][6] = -0.34857292408604584
self.W[14][6] = -0.58353859501523964; self.W[15][6] = -0.41258775067250342
self.W[16][6] = 0.91182517839270993; self.W[17][6] = -0.56916166564089354
self.W[18][6] = -1.0285604223454949 #bias weight input should be 1.0

self.W[0][7] = -0.32865925594153583; self.W[1][7] = 0.04942365443898445
self.W[2][7] = 0.94576664098391583; self.W[3][7] = -0.52058188611049716
self.W[4][7] = 0.34173019628887918; self.W[5][7] = 0.23316279649833077
self.W[6][7] = 0.93354218924489529; self.W[7][7] = -0.36723992736160 16
self.W[8][7] = 0.24492040865298623; self.W[9][7] = 0.62309764743750939
self.W[10][7] = -0.31738646556078642; self.W[11][7] = 0.49240143356911215
self.W[12][7] = -0.63613804743008662; self.W[13][7] = 0.27255090370977308

```
self.W[14][7] = -0.077490270085429441; self.W[15][7] = 0.03996644688196864
self.W[16][7] = -0.42607929700787811; self.W[17][7] = 0.070260106536832997
self.W[18][7] = 0.68278617148868181    #bias weight input should be 1.0

self.W[0][8] = -0.5203133183715809; self.W[1][8] = 0.76526828167302097
self.W[2][8] = 0.11362124877625604; self.W[3][8] = 0.93936007101853969
self.W[4][8] = -0.32325776716962157; self.W[5][8] = -0.50373426830327472
self.W[6][8] = -0.61124578984982036; self.W[7][8] = -0.55151966342108183
self.W[8][8] = -0.50104432378214458; self.W[9][8] = -0.30459007736977906
self.W[10][8] = -0.3159522940418959; self.W[11][8] = -0.065342188976498211
self.W[12][8] = 0.39061159628437425; self.W[13][8] = 0.59170422967153369
self.W[14][8] = -0.16956740248484886; self.W[15][8] = 0.18794488956438776
self.W[16][8] = -0.34436713394629842; self.W[17][8] = 0.63513932853507671
self.W[18][8] = 0.30307186938747249    #bias weight input should be 1.0

self.W[0][9] = -0.8275124467384023; self.W[1][9] = -0.11677639936330871
self.W[2][9] = -0.1251652096057006; self.W[3][9] = -0.34447644211000494
self.W[4][9] = 0.44231016923933497; self.W[5][9] = -0.67835978699981769
self.W[6][9] = 0.10671669828894725; self.W[7][9] = 0.052493351739184235
self.W[8][9] = -0.13220081875069595; self.W[9][9] = -0.37290173453154851
self.W[10][9] = 0.037026514129265595; self.W[11][9] = -0.38829556664334314
self.W[12][9] = -0.41969064484146179; self.W[13][9] = 1.0370135682327706
self.W[14][9] = 0.72233117331089669; self.W[15][9] = -0.26787152887521748
self.W[16][9] = -0.032418233516579437; self.W[17][9] = -0.47082294426757276
self.W[18][9] = 0.58984303347455413    #bias weight input should be 1.0

self.W[0][10] = 0.99545420020183517; self.W[1][10] = 0.40670899831678181
self.W[2][10] = 0.11853073510231668; self.W[3][10] = 0.58812453777427598
self.W[4][10] = -0.79645600422265672; self.W[5][10] = 0.25972144416010789
self.W[6][10] = -0.74823811652818473; self.W[7][10] = 0.60024217417752057
self.W[8][10] = -0.0073119157875114237; self.W[9][10] = 0.84124958610319833
self.W[10][10] = -0.2617949002805095; self.W[11][10] = 0.64006977894777428
self.W[12][10] = 0.94779267061153l5; self.W[13][10] = -0.29951602470691668
self.W[14][10] = 0.30016030289901718; self.W[15][10] = -0.83346922323500006
self.W[16][10] = 0.17169493427772073; self.W[17][10] = 0.40107106183219271
self.W[18][10] = 0.70903533284002751    #bias weight input should be 1.0

self.W[0][11] = -1.142759022542396; self.W[1][11] = 0.449854142515745 63
self.W[2][11] = 0.3895513876502969; self.W[3][11] = -1.226383084875748
self.W[4][11] = -0.92868023640950426; self.W[5][11] = -0.49184381233707225
self.W[6][11] = 0.17925844190885934; self.W[7][11] = -0.20505890929724421
self.W[8][11] = 0.64675932461962349; self.W[9][11] = 0.14682528315075502
self.W[10][11] = 0.035955907391130484; self.W[11][11] = -0.24746822575992516
self.W[12][11] = -0.50773043572067322; self.W[13][11] = 0.24967556622437737
self.W[14][11] = 0.80942581518738244; self.W[15][11] = 0.69574565324455129
self.W[16][11] = 0.23778917275425218; self.W[17][11] = 0.89204034325895742
```

```
self.W[18][11] = 0.2218448568058044   #bias weight input should be 1.0

self.W[0][12] = -0.35511846140043241; self.W[1][12] = 0.70733180758484104
self.W[2][12] = -0.83165126184425742; self.W[3][12] = -0.83504960919917026
self.W[4][12] = -0.13755256747487241; self.W[5][12] = -0.52966103620956229
self.W[6][12] = 0.25071078472815855; self.W[7][12] = -0.35216098305186072
self.W[8][12] = 0.088542557230076688; self.W[9][12] = -1.1040221735380804
self.W[10][12] = 0.79594009769706098; self.W[11][12] = -0.73714848198026295
self.W[12][12] = -0.18180847746449641; self.W[13][12] = 0.41331841770555355
self.W[14][12] = 0.41428659784606314; self.W[15][12] = -0.4290960896492258
self.W[16][12] = -0.98897305155024584; self.W[17][12] = 0.78215239795834623
self.W[18][12] = -0.44364199938191162   #bias weight input should be 1.0

self.W[0][13] = 0.79858959493477089; self.W[1][13] = 0.10650095639849158
self.W[2][13] = 0.41879177374855703; self.W[3][13] = 1.0263932028577394
self.W[4][13] = 0.189570080155397; self.W[5][13] = -0.44376619219939994
self.W[6][13] = -0.60203148870373557; self.W[7][13] = 0.74519204084468549
self.W[8][13] = 0.20937947312546459; self.W[9][13] = -0.73403570501855497
self.W[10][13] = 0.030778866771470657; self.W[11][13] = 0.28322753361566022
self.W[12][13] = 0.92880385369204232; self.W[13][13] = 0.1644240293137085
self.W[14][13] = -0.21608287824017328; self.W[15][13] = -0.2904478515294443
self.W[16][13] = -0.41154041855238949; self.W[17][13] = 0.90293535522249624
self.W[18][13] = 0.97015377694600791   #bias weight input should be 1.0

self.W[0][14] = -1.0325407768158865; self.W[1][14] = -0.84527794204417972
self.W[2][14] = -0.25248895386672582; self.W[3][14] = 0.47151219855652071
self.W[4][14] = -0.94815743730612323; self.W[5][14] = 0.067206226767283619
self.W[6][14] = 0.54728649621049807; self.W[7][14] = -0.87468384013164791
self.W[8][14] = -0.0083579697762564686; self.W[9][14] = 0.74901199144024511
self.W[10][14] = -0.63222006168505462; self.W[11][14] = -0.87475753047840932
self.W[12][14] = 0.90162993286440094; self.W[13][14] = -0.11257067471748695
self.W[14][14] = -0.27838527717268613; self.W[15][14] = 0.95224921487717162
self.W[16][14] = 0.50084256089794099; self.W[17][14] = -0.71743881771230811
self.W[18][14] = -0.02701900591046871   #bias weight input should be 1.0

self.W[0][15] = 1.0437741273389674; self.W[1][15] = -0.45408494721878151
self.W[2][15] = 0.96511020810437909; self.W[3][15] = -0.30063151326050935
self.W[4][15] = -0.071082781756073923; self.W[5][15] = 0.2447287444213701
self.W[6][15] = -0.24195063780165757; self.W[7][15] = 0.98824904641780897
self.W[8][15] = 0.74073183617769423; self.W[9][15] = 0.43863706340778019
self.W[10][15] = -1.0108726386238427; self.W[11][15] = -0.79646911633394357
self.W[12][15] = -0.36001428038607081; self.W[13][15] = 0.17255191773894921
self.W[14][15] = -0.16546627399110897; self.W[15][15] = -0.3996833211136836
self.W[16][15] = -1.2185776823559316; self.W[17][15] = -0.1455316758747702
self.W[18][15] = 1.1403808043303105   #bias weight input should be 1.0
```

```
self.W2[0][0] = -0.84028171889997116; self.W2[1][0] = -0.43346076499958708
self.W2[2][0] = -0.43557589480677411; self.W2[3][0] = -0.42513219690958287
self.W2[4][0] = 0.54188493979188723; self.W2[5][0] = -0.046737792182397153
self.W2[6][0] = -0.80478664818881229; self.W2[7][0] = -0.678851216176377
self.W2[8][0] = 0.71149222702874249; self.W2[9][0] = 0.68341599319600177
self.W2[10][0] = 1.0328752945835469; self.W2[11][0] = 0.24740667798727475
self.W2[12][0] = -0.2469023592420069; self.W2[13][0] = 0.508095168051796
self.W2[14][0] = -0.69387411534727783; self.W2[15][0] = 0.19338083305716081
self.W2[16][0] = 0.18211612650330075    #bias weight input should be 1.0

self.W2[0][1] = 0.2859958155039441; self.W2[1][1] = 0.24091476574654414
self.W2[2][1] = 0.91115699781689941; self.W2[3][1] = 0.48388496460003888
self.W2[4][1] = -0.68637080910887738; self.W2[5][1] = 0.61678116159010321
self.W2[6][1] = 0.071795625009126882; self.W2[7][1] = -0.73207375760099258
self.W2[8][1] = 0.6556064256037778; self.W2[9][1] = -0.44088680852652473
self.W2[10][1] = -0.20501788340358035; self.W2[11][1] = -0.4010598542444288
self.W2[12][1] = -0.45119284181746144; self.W2[13][1] = 0.52587578563884863
self.W2[14][1] = -0.22088901355724097; self.W2[15][1] = 0.2495482636642444
self.W2[16][1] = -0.60347877573598951    #bias weight input should be 1.0

self.W2[0][2] = 0.42336720355483193; self.W2[1][2] = 0.50245942687953626
self.W2[2][2] = 0.21654723337885157; self.W2[3][2] = 0.70531360649670838
self.W2[4][2] = 0.093535694516742818; self.W2[5][2] = -0.21420036356255232
self.W2[6][2] = -0.012639507473030611; self.W2[7][2] = 0.31554596948648805
self.W2[8][2] = -0.0040929337148137854; self.W2[9][2] = -0.17044839540087706
self.W2[10][2] = 0.46951908908293116; self.W2[11][2] = -0.66754027180472342
self.W2[12][2] = 0.82473208826382194; self.W2[13][2] = -0.1571156431250397
self.W2[14][2] = -0.42213152740242382; self.W2[15][2] = 0.79329857749148425
self.W2[16][2] = 0.80557575135338377    #bias weight input should be 1.0

self.W2[0][3] = -0.13255563062284348; self.W2[1][3] = 0.37810476302366636
self.W2[2][3] = 0.21070959566965541; self.W2[3][3] = -0.89366749130281953
self.W2[4][3] = 1.0078487477830862; self.W2[5][3] = 0.42900826466769421
self.W2[6][3] = 0.39769863416066875; self.W2[7][3] = -0.49379617511626256
self.W2[8][3] = 0.26323002509449323; self.W2[9][3] = -0.37429078671305493
self.W2[10][3] = 0.86815937993400716; self.W2[11][3] = -0.59414843110057125
self.W2[12][3] = 0.51956225729714856; self.W2[13][3] = -0.34767642086198647
self.W2[14][3] = -1.0664791956925401; self.W2[15][3] = 0.81194836042924168
self.W2[16][3] = 0.38600602910012766    #bias weight input should be 1.0

self.W2[0][4] = -0.7852457933457988; self.W2[1][4] = 0.67182369199536496
self.W2[2][4] = 0.11976172539016033; self.W2[3][4] = -0.35345828007455571
self.W2[4][4] = -0.75884001297513415; self.W2[5][4] = -0.68270928953850274
self.W2[6][4] = 0.039984026585529499; self.W2[7][4] = 0.1324556886239189
self.W2[8][4] = -0.42219247413963362; self.W2[9][4] = 0.76451311676056533
self.W2[10][4] = 0.67287618465966093; self.W2[11][4] = 0.17620257431174735
```

```
        self.W2[12][4] = -0.37423290298627587; self.W2[13][4] = 0.15449217725083536
        self.W2[14][4] = 0.15546713985527782; self.W2[15][4] = 0.94462533981671326
        self.W2[16][4] = 0.52053670319683165    #bias weight input should be 1.0

        self.W2[0][5] = -0.11383317674524207; self.W2[1][5] = 1.093880403742064
        self.W2[2][5] = 0.48574982685208123; self.W2[3][5] = -0.36562169083116408
        self.W2[4][5] = 0.8476825029450753; self.W2[5][5] = -0.2273487774476374
        self.W2[6][5] = -0.84103370298577607; self.W2[7][5] = -0.47561685116962277
        self.W2[8][5] = 0.76334113447610374; self.W2[9][5] = 0.5048639068148526
        self.W2[10][5] = -0.53656874325571335; self.W2[11][5] = -0.33513742916677347
        self.W2[12][5] = -0.28172906506309481; self.W2[13][5] = -0.76272398129498198
        self.W2[14][5] = -0.66025788802885732; self.W2[15][5] = 0.95701289266244449
        self.W2[16][5] = -0.3592191351002838    #bias weight input should be 1.0

        self.W2[0][6] = -0.21764607397928706; self.W2[1][6] = 0.75056281843678718
        self.W2[2][6] = -0.55413003683237416; self.W2[3][6] = -0.13285829175998887
        self.W2[4][6] = 0.58529457481651215; self.W2[5][6] = -0.7624180695963737
        self.W2[6][6] = 0.31736963218013603; self.W2[7][6] = -0.9402512575105112
        self.W2[8][6] = -0.6711298052291685 4; self.W2[9][6] = -0.7235067875934823
        self.W2[10][6] = -0.26022571343166184; self.W2[11][6] = -0.43886863821482747
        self.W2[12][6] = 0.3063464033973422; self.W2[13][6] = -0.58939225217425462
        self.W2[14][6] = 0.45724366645921521; self.W2[15][6] = 0.5685444957630944
        self.W2[16][6] = -0.88450826792892168    #bias weight input should be 1.0

        self.wts = [self.W, self.W2] #list of weight arrays for each layer; in order
                    # [W, W2, W3] for three hidden layers


        #weights from hidden to output

        self.WO[0] = -0.26706611706223854
        self.WO[1] = -0.42003016388263759
        self.WO[2] = 0.72028255111376516
        self.WO[3] = 0.28335883323926864
        self.WO[4] = -0.89717920199668166
        self.WO[5] = -0.49025758877601794
        self.WO[6] = -0.38930986874947926
        self.WO[7] = 0.30361700984309659 #bias sign change ! to subtract threshold



    def scaler(self):

        ''' linear scaling of input values; -9999 is missing value '''

        missing = [0.27413464591933939, 0.30335820895522386, 0.31809701492537301,
```

```
        0.26026119402985076, 0.37654065907577805, 0.65600816582363053,
        0.65964013022874357, 0.50367098331870064, 0.37765094021418316,
        0.4680048264547062, 0.50156899600184768, 0.58077275397528705 ]

# slope and intercept for scaling inputs

linear_eq= {0:(0.021276595744680851, -0.34042553191489361), 1:(0.025, -0.3),
        2:(0.020833333333333332, -0.4375), 3:(0.03125, -0.125),
        4:(0.011224516139170531, -0.67367525454396482),
        5:(0.027361802376646153, 0.50862854437947536),
        6:(0.028418294561306793, 0.30574390569673132),
        7:(0.14705882352941174, 0.5911764705882353),
        8:(0.14124293785310735, 0.43926553672316382),
        9:(0.053361792956243326, 0.50266808964781207),
        10:(0.053361792956243326, 0.50266808964781207),
        11:(0.033355570380253496, 0.59239492995330223) }

categ_eq = {0:0.45149253731343286, 1:0.39925373134328357,
        2:0.48134328358208955, 3:0.15298507462686567,
        4:0.089552238805970144, 5:0.55970149253731338}

lineqs = len(missing)

for i in range(lineqs):

    if self.pattern[i] == -9999:
        self.pattern[i] = missing[i]
    else:
        self.pattern[i] = self.pattern[i] * linear_eq[i][0] + linear_eq[i][1]


for i in range(len(categ_eq)):

    if self.pattern[i + lineqs] == 0:

        self.pattern[i + lineqs] = categ_eq[i]

    elif self.pattern[i + lineqs] == 1:

        self.pattern[i + lineqs] = 0

    else:

        self.pattern[i + lineqs] = 1
```

```
    #print self.pattern


def activ(self, x):

    ''' sigmoidal activation: inputs to hidden '''

    if x > 100.0: x = 1.0
    if x < -100.0: x = -1.0

    e1 = math.exp(x)
    e2 = math.exp(-x)

    #print x, e1, e2

    return (e1 - e2) / (e1 + e2)


def layerX(self, nh, invalues, W, activ): #number hidden nodes in layer,
                                # of inputs, Wt matrix, activation func

    ''' from inputs to hidden layer '''


    hidden = matrixmultiply(invalues, W)

    #print hidden

    for i in range(len(hidden)):

        hidden[i] = activ(hidden[i])

        #print hidden[i]

    hidden2 = zeros((nh + 1), Float32)

    hidden2[nh] = 1.0  #bias or threshold input

    for i in range(nh):

        hidden2[i] = hidden[i]

    return hidden2


def layer_out(self):
```

```
        self.pattern.append(1.0) #bias or threshold input

        inputs = self.pattern

        for i in range(self.N_layers):


            inputs = self.layerX(self.N_hidden[i], inputs, self.wts[i], self.afunc[i])


        return matrixmultiply(inputs, self.WO)



    def out_scale(self, x):

        ''' inverse scaling to get LAI output '''

        self. prediction = (x + 0.099788683247846094)/ 0.23868893546020067


    def predict(self):

        self.scaler() # scale input pattern
        x = self.layer_out() #apply weights and activation function
        self.out_scale(x) # predict LAI (self.prediction)




if __name__ == '__main__':

    test = Predict_LAI()
    test.predict()
    print "LAI for test pattern should be 1.41547"
    print "This program calculates: "
    print test.prediction
    print ' '
    test.pattern = []
    for i in range(18):
        x = raw_input(test.in_labels[i])
        x = float(x)
        test.pattern.append(x)
    print ' '
```

```
test.predict()
print 'LAI = ',test.prediction
zzz = raw_input('DONE')
```

LIST OF REFERENCES

Anselin L. (2003) GEODA 0.9 User's Guide. University of Illinois, Urbana-Champaign, IL

Asner G.P. & Wessman C.A. (1997) Scaling PAR Absorption from the Leaf to Landscape Level in Spatially Heterogeneous Ecosystems. *Ecological Modelling*, *103*, 81-97

Birth G.S. & Mcvey G.R. (1968) Measuring Color of Growing Turf with a Reflectance Spectrophotometer. *Agronomy Journal*, *60*, 640-649

Chicago Climate Exchange (2005) Carbon Financial Instrument Market Data http://www.chicagoclimatex.com/trading/stats/daily/index.html: May 30, 2005

Clark K.L., Cropper W.P. & Gholz H.L. (2001) Evaluation of Modeled Carbon Fluxes for a Slash Pine Ecosystem: SPM2 Simulations Compared to Eddy Flux Measurements. *Forest Science*, *47*, 52-59

Cohen W.B., Maiersperger T.K., Gower S.T. & Turner D.P. (2003) An Improved Strategy for Regression of Biophysical Variables and Landsat ETM+ Data. *Remote Sensing of Environment*, *84*, 561-571

Crist E.P. & Cicone R.C. (1984) A Physically-Based Transformation of Thematic Mapper Data - the Tm Tasseled Cap. *IEEE Transactions on Geoscience and Remote Sensing*, *22*, 256-263

Cropper W.P. (2000) SPM2: A Simulation Model for Slash Pine (Pinus elliottii) Forests. *Forest Ecology and Management*, *126*, 201-212

Cropper W.P. & Gholz H.L. (1993) Simulation of the Carbon Dynamics of a Florida Slash Pine Plantation. *Ecological Modelling*, *66*, 231-249

Curran P.J., Dungan J.L. & Gholz H.L. (1992) Seasonal LAI in Slash Pine Estimated with Landsat Tm. *Remote Sensing of Environment*, *39*, 3-13

Doran, J. 2003. Landmark Emissions Exchange Launched in Chicago. *The Times*. London. Oct. 1, pg 75

Eklundh L., Hall K., Eriksson H., Ardo J. & Pilesjo P. (2003) Investigating the Use of Landsat Thematic Mapper Data for Estimation of Forest Leaf Area Index in Southern Sweden. *Canadian Journal of Remote Sensing*, *29*, 349-362

ESRI (2003) ArcMap 8.3. ESRI. Redlands CA.

Fang H.L. & Liang S.L. (2003) Retrieving Leaf Area Index with a Neural Network Method: Simulation and Validation. *IEEE Transactions on Geoscience and Remote Sensing*, *41*, 2052-2062

Fassnacht K.S., Gower S.T., MacKenzie M.D., Nordheim E.V. & Lillesand T.M. (1997) Estimating the Leaf Area Index of North Central Wisconsin Forests Using the Landsat Thematic Mapper. *Remote Sensing of Environment*, *61*, 229-245

Gholz H.L., Vogel S.A., Cropper W.P., McKelvey K., Ewel K.C., Teskey R.O. & Curran P.J. (1991) Dynamics of Canopy Structure and Light Interception in Pinus-Elliottii Stands, North Florida. *Ecological Monographs*, *61*, 33-51

Gobron N., Pinty B. & Verstraete M.M. (1997) Theoretical Limits to the Estimation of the Leaf Area Index on the Basis of Visible and Near-infrared Remote Sensing Data. *IEEE Transactions on Geoscience and Remote Sensing*, *35*, 1438-1445

Gower S.T., Kucharik C.J. & Norman J.M. (1999) Direct and Indirect Estimation of Leaf Area Index, f(APAR), and Net Primary Production of Terrestrial Ecosystems. *Remote Sensing of Environment*, *70*, 29-51

Hintze J. (2001) Number Cruncher Statstitical Systems (NCSS). Kaysville, UT

Hodges A.W., Mulkey W.D., Alavalapati J.R., Carter D.R. & Kiker C.F. (2005) Economic Impacts of the Forest Industry in Florida, 2003. In, p. 47. IFAS, University of Florida, Gainesville, FL

Holben B., Kimes D. & Fraser R.S. (1986) Directional Reflectance Response in AVHRR Red and Near-Ir Bands for 3 Cover Types and Varying Atmospheric Conditions. *Remote Sensing of Environment*, *19*, 213-236

Huang C., Wylie B., Yang L., Homer C. & Zylstra G. (2002) Derivation of a Tasselled Cap Transformation Based on Landsat 7 At-satellite Reflectance. *International Journal of Remote Sensing*, *23*, 1741-1748

Huete A.R. (1988) A Soil-Adjusted Vegetation Index (SAVI). *Remote Sensing of Environment*, *25*, 295-309

Jensen J.R. (2000) *Remote Sensing of the Environment : An Earth Resource Perspective*. Prentice Hall, Upper Saddle River, N.J.

Jensen J.R., Qiu F. & Ji M.H. (1999) Predictive Modeling of Coniferous Forest Age Using Statistical and Artificial Neural Network Approaches Applied to Remote Sensor Data. *International Journal of Remote Sensing*, *20*, 2805-2822

Karl T.R. & Knight R.W. (1985) *Atlas of the Palmer Hydrological Drought Indices (1931-1983) for the contiguous United States*. National Environmental Satellite Data and Information Service, Asheville, N.C.

Leica Geosystems GIS and Mapping. (2003) ERDAS IMAGINE 8.7. Atlanta, GA

Lucas R.M., Milne A.K., Cronin N., Witte C. & Denham R. (2000) The Potential of Synthetic Aperture Radar (SAR) for Quantifying the Biomass of Australia's Woodlands. *Rangeland Journal*, *22*, 124-140

Martin T.A. & Jokela E.J. (2004) Developmental Patterns and Nutrition Impact Radiation Use Efficiency Components in Southern Pine Stands. *Ecological Applications*, *14*, 1839-1854

Mehrotra K., Mohan C.K. & Ranka S. (2000) *Elements of Artificial Neural Networks*. MIT Press, Cambridge, MA.

National Climatic Data Center (2005) Palmer Hydrological Drought Index Florida-Division 2: 1895 - 2005 Monthly Averages http://climvis.ncdc.noaa.gov/cgi-bin/ginterface: May 12, 2005

Prestemon J.P. & Abt R.C. (2002) Timber Products: Supply and Demand. In: *Southern Forest Resource Assessment* (eds. Wear DN & Greis JG), pp. 299-325. Southern Research Station, USDA Forest Service, Asheville, N.C.

Raffy M., Soudani K. & Trautmann J. (2003) On The Variability of the LAI of Homogeneous Covers with Respect to the Surface Size and Application. *International Journal of Remote Sensing*, *24*, 2017-2035

Ramsey E.W. & Jensen J.R. (1996) Remote Sensing of Mangrove Wetlands: Relating Canopy Spectra to Site-specific Data. *Photogrammetric Engineering and Remote Sensing*, *62*, 939-948

Reich P.B., Turner D.P. & Bolstad P. (1999) An Approach to Spatially Distributed Modeling of Net Primary Production (NPP) at the Landscape Scale and its Application in Validation of EOS NPP Products. *Remote Sensing of Environment*, *70*, 69-81

Rouse J.W., Haas R.H., Schell J.A. & Deering D.W. (1973) Monitoring Vegetation Systems in the Great Plains with ERTS. In: *3rd ERTS Symposium*, NASA SP-351, Vol 1, pp. 48-62

Running S.W., Peterson D.L., Spanner M.A. & Teuber K.B. (1986) Remote-Sensing of Coniferous Forest Leaf-Area. *Ecology*, *67*, 273-276

Sader S.A., Bertrand M. & Wilson E.H. (2003) Satellite Change Detection of Forest Harvest Patterns on an Industrial Forest Landscape. *Forest Science*, *49*, 341-353

Sampson D.A., Vose J.M. & Allen H.L. (1998) A Conceptual Approach to Stand Management Using Leaf Area Index as the Integral of Site Structure, Physiological Function, and Resource Supply. In: *Proceedings of the ninth biennial southern silvicultural research conference* (ed. Waldrop TA), pp. 447-451. U. S. Department of Agriculture, Forest Service, Southern Research Station, Clemson, S. C.

Smith M.L., Ollinger S.V., Martin M.E., Aber J.D., Hallett R.A. & Goodale C.L. (2002) Direct Estimation of Above Ground Forest Productivity Through Hyperspectral Remote Sensing of Canopy Nitrogen. *Ecological Applications*, *12*, 1286-1302

Soudani K., Trautmann J. & Walter J.M.N. (2002) Leaf Area Index and Canopy Stratification in Scots pine (Pinus sylvestris L.) Stands. *International Journal of Remote Sensing*, *23*, 3605-3618

Starr G., Martin T.A., Binford M.W., Gholz H.L. & Genec L. (2003) Integration of Carbon Dynamics From Leaf to Landscape in Florida Pine Forest. ESA Report #140. Ecological Society of America, Savannah, GA

StatSoft Inc. (2004) STATISTICA. Tulsa, OK

Stenberg P., Nilson T., Smolander H. & Voipio P. (2003) Gap Fraction Based Estimation of LAI in Scots Pine Stands Subjected to Experimental Removal of Branches and Stems. *Canadian Journal of Remote Sensing*, *29*, 363-370

Swindle B.F., Neary D.G., Comerford N.B., Rockwood D.L. & Blakeslee G.M. (1988) Fertilization and Competition Control Accelerate Early Southern Pine Growth on Flatwoods. *Southern Journal of Applied Forestry*, *12*, 116-121

Tans P.P. & White J.W.C. (1998) The Global Carbon Cycle—In Balance, With A Little Help From the Plants. *Science*, *281*, 183-184

Teskey R.O., Gholz H.L. & Cropper W.P. (1994) Influence of Climate and Fertilization on Net Photosynthesis of Mature Slash Pine. *Tree Physiology*, *14*, 1215-1227

Trishchenko A.P., Cihlar J. & Li Z.Q. (2002) Effects of Spectral Response Function on Surface Reflectance and NDVI Measured With Moderate Resolution Satellite Sensors. *Remote Sensing of Environment*, *81*, 1-18

Turner D.P., Guzy M., Lefsky M.A., Ritts W.D., VAN Tuyl S. & Law B.E. (2004a) Monitoring Forest Carbon Sequestration with Remote Sensing and Carbon Cycle Modeling. *Environmental Management*, *33*, 457-466

Turner D.P., Ollinger S.V. & Kimball J.S. (2004b) Integrating Remote Sensing and Ecosystem Process Models for Landscape- To Regional-Scale Analysis of the Carbon Cycle. *Bioscience*, *54*, 573-584

Waring R.H. & Running S.W. (1998) *Forest Ecosystems : Analysis At Multiple Scales.* Academic Press, San Diego

Wood G.A., Taylor J.C. & Godwin R.J. (2003) Calibration Methodology for Mapping Within-field Crop Variability Using Remote Sensing. *Biosystems Engineering*, *84*, 409-423

BIOGRAPHICAL SKETCH

Douglas Allen Shoemaker was born in Washington, DC, on August 26, 1962, first of three sons to Wayne B. and Joanne Shoemaker. Raised in the nearby suburbs of Maryland, Douglas cultivated a love for the outdoors on frequent hunting, hiking and fishing trips with his father and brothers. On his entry to the University of Maryland in 1980, he brought with him college credits earned through advanced placement English and biology testing while still in high school. Originally a zoology major, his interests changed and after two years he left UM to drift through a series of jobs including elephant keeper, construction worker and semiprofessional bicycle racer. Douglas was nearly killed in a 1988 boating accident off of St. Croix, U.S.V.I., an experience that dramatically changed his life. Returning to the U.S.A. he promptly undertook a career in retail sales, an occupation he maintained for the next 12 years. During this period Douglas married Kathryn Jean Goody of Andover NH and had the first of two daughters, Brook Hanna. In 2001 Douglas left his position and returned to finish his education, entering the University of Massachusetts majoring in biology and geographic information science. Graduating with a Bachelor of Science degree *summa cum laude*, Douglas arrived at the University of Florida's School of Forest Resources and Conservation in 2003 to work with Dr. Wendell Cropper, Jr. modeling forest processes using remote sensing